Thesis for the Degree of Doctor of Philosophy

Regulation of macrophage polarization switch using *Pyropia yezoensis* glycoprotein and protective mechanisms in animal liver injury model

by

Jeong Wook Choi

Department of Food and Life Science

The Graduate School

Pukyong National University

February 2016

Regulation of macrophage polarization switch using *Pyropia yezoensis* glycoprotein and protective mechanisms in animal liver injury model

(김 단백질의 대식세포 표현형 전환과 동물 간 손상 모델에서의 보호 메커니즘)

Advisor : Prof. Taek Jeong Nam

by

Jeong Wook Choi

A thesis submitted in partial fulfillment of the requirements for the degree of

Doctor of Philosophy

in Department of Food and Life Science, The Graduate School, Pukyong National University

February 2016

Regulation of macrophage polarization switch using *Pyropia yezoensis* glycoprotein and protective mechanisms in animal liver injury model

A dissertation
by
Jeong Wook Choi

Approved by:

(Chairman) Jae-Sue Choi

(member) Eun-Soon Lyu

(member) Dong-Hyun Ahn

(member) Dong-Soo Kim

(member) Taek-Jeong Nam

February 26, 2016

CONTENTS

Abbreviations

AP-1 : activator protein-1
ARG1 : arginase1
BSA : bovine serum albumin
BW : body weight
CAT : catalase
CCL2 : chemokine (C-C motif) ligand 2
CON : control
COX-2 : cyclooxygenase-2
CYP2E1 : cytochrome P450 2E1
DCF-DA 2',7'-dichlorofluorescenin diacetate
D-GalN : D-Galactosamine
DTT : 1,4-dithiothreitol
EDTA : trypsis-ethylendiamine tetraacetic acid
EGTA : ethylene glycol bis-(β-aminoethylether)-N,N,N',N'-tetra acetic acid
ERK : extracellular signal-regulated kinase
FBS : fetal bovine serum
FIZZ1 : resistin-like-α
GOT : glutamate oxaloacetic transaminase
GPT : glutamate pyruvic transaminase
GSH : glutathione
GSH-px : glutathione peroxidase
GST : glutathione-S-transferase
HO-1 : heme oxygenase-1
IFN-γ : interferon-γ
IL-10 : interleukin-10
IL-1β : interleukin-1β
IL-6 : interleukin-6
iNOS : inducible NO synthase
IRFs : interferon-recognition factor

JNK : c-Jun N-terminal kinases
kDa : kilodalton
LDH : lactate dehydrogenase
LPS : lipopolysaccharide
MAPK : mitogen-activated protein kinase
MTS : 3-(4,5-dimethylthiazol-2-yl)-5-(3-carboxymethoxiphenyl)-2-(4-sulfophenyl)-2H-tetraziloum
MW : molecular weight
NF-κB : nuclear factor κB
NO : nitrogen oxide
NOS-2 : nitric oxide synthase-2
Nqo1 : NADPH quinine oxidoreductase 1
Nrf2 : nuclear factor erythroid 2-related factor 2
PBS : phosphate-buffered saline
PMSF : phenylsufonyl fluoride
PYGP : *Pyropia yezoensis* glycoprotein
ROS : reactive oxygen species
RPMI 1640 : rosewell park memorial institute 1640
RT : room temperature
SFM : serum free medium
SOD : superoxide dismutase
STAT3 : signal transducers and activators of transcription3
STAT6 : signal transducers and activators of transcription6
TBARS : thiobarbituric acid reactive substances
TBS-T : tris-buffered saline tween-20
TLR4 : toll-like receptor 4
TNF-α : tumor necrosis factor-α
Ym1 : chitinase 3-like 3

Regulation of macrophage polarization switch using *Pyropia yezoensis* glycoprotein and protective mechanisms in animal liver injury model

최 정 욱

부경대학교 대학원 식품생명과학과

요 약

염증반응은 신체의 외부감염에 대한 방어 작용과 손상에 대한 회복에 중요한 역할을 하는 것으로 알려져 있으며, 이러한 염증반응에 관여하는 대식세포는 M1(classically activation), M2(alternatively activation) 표현형에 따라 각각의 자극반응에서 다른 역할을 수행하게 된다. M1 표현형의 대식세포는 전염증성 싸이토카인을 분비하게 되며 산화질소와 활성산소 매개물질을 생성하게 된다. 반면, M2 표현형의 대식세포는 M1 표현형의 대식세포를 M2 표현형으로 전환시키며 항염증 작용 및 손상된 조직의 회복을 촉진시킨다. 본 연구에서는 방사무늬 김(*Pyropia yezoensis*)에서 분리한 단백질을 이용하여 대식세포의 M1, M2 활성에 미치는 영향과 그와 연관된 질병모델에서 김 단백질의 영향에 대하여 확인하였다. 먼저 김 단백질이 RAW 264.7 마우스 대식세포의 M1 활성에 미치는 영향을 알아보기 위해서 LPS를 자극제로 이용한 모델을 사용하였다. MTS assay 결과 김 단백질과 LPS는 대식세포의 생존율에 영향을 미치지 않았으며, RAW 264.7 대식세포의 M1 표현형에서 생성되어지는 NO, ROS의 생성을 김 단백질이 효과적으로 억제하는 것을 확인하였다. Western blot과 RT-PCR을 통하여 M1, M2 표현형 마커를 관찰한 결과 김 단백질이 LPS 자극으로 유도되어진 IL-6, IL-1β, TNF-α, IFN-γ, NOS-2, SOCS3, M1 표현형 마커의 발현을 억제하는 것이 확인되었고, M2 표현형의 마커인 ARG1, Ym1, FIZZ1, IL-10의 발현이 유의적으로 증가하는 것이 관찰되었다. M1 표현형과 M2 표현형에서는 세포외부의 CD항원 발현에도 차이가 발견되는데 M2 표현형에서 특이적으로 발현되어지는 CD163, CD206의 발현은 김 단백질을 처리하였을 때 증가되는 것으로 확인되었다. 이러한 대식세포 표현형 활성에는 다양한 전사인자가 관여하는데 이중 STAT3, STAT6 전사인자의 변화를 관찰한 결과 김 단백질에 의하여 인산화되어 활성이 증가하였으며, STAT6 전사인자로 매개되어지는 PPARγ, KLF4의 발현이 증가되는 것으로 확인되었다. 반면, M1활성을 촉진하는 NFκB와 AP-1 전사인자의 핵내 유입은 감소하는 것으로 나타났다. STAT3, STAT6의 siRNA를 이용하여 STAT3, 6 전

사인자를 knock down시킨 결과에서는 김 단백질을 처리했음에도 ARG1, Ym1, FIZZ1, CD206, CD163 M2 표현형 마커의 발현이 증가하지 않는 것이 관찰되었다.

김 단백질의 간 손상모델에서의 효과를 관찰하기 위하여 Hepa 1c1c7 마우스 간암세포에 D-galactosamine(D-GalN)을 처리하여 독성을 유발하는 모델을 이용하여 생리적 변화를 관찰하였다. 그 결과, D-GalN에 노출로 저하된 Hepa 1c1c7 세포의 생존율이 김 단백질을 처리함으로써 회복되어지는 것이 MTS, LDH assay를 통하여 확인되었다. D-GalN으로 유발되는 산화적 스트레스로 인하여 상승된 TBARS가 김 단백질 농도 유의적으로 감소하였으며 D-GalN으로 저해된 SOD, CAT, GST 항산화 효소의 활성이 김 단백질 농도 유의적으로 회복되어졌다. D-GalN으로 인한 세포의 독성은 MAPK 경로의 활성화가 중요한 역할을 담당하는 것으로 알려져 있는데, 김 단백질을 동시처리함으로써 MAPK의 활성화가 유의적으로 감소하는 결과가 나타났다. 또한 산화적 스트레스의 억제를 담당하는 Nrf2 전사인자의 발현을 김 단백질이 촉진시키며 Nrf2로 매개되어지는 Nqo1, GST, HO-1 단백질의 발현 역시 증가함이 확인되었다.

In vitro 실험에서의 결과를 토대로 *in vivo*에 적용하여 그 효과를 검증하기 위해 sprague dawley rat에 D-GalN과 LPS를 동시에 처리하는 모델을 사용하였다. D-GalN/LPS으로 인하여 rat의 간 조직이 손상되었는지 확인하기 위하여 혈청 GOT, GPT 수치를 측정한 결과 D-GalN/LPS가 간 손상을 유발한 것이 확인되어졌으며 김 단백질로 인하여 회복되는 것으로 나타났다. 또한 간 조직의 산화적 스트레스를 파악하기 위해 TBARS와 항산화 효소인 CAT, GST, GSH효소를 측정한 결과 D-GalN/LPS으로 상승된 TBARS는 김 단백질을 함께 투여한 군에서 저해되었으며 항산화효소인 CAT, GST, GSH의 감소는 김 단백질을 투여함으로써 회복되어졌다. D-GalN/LPS의 독성 경로에 밀접한 역할을 하는 MAPK 인산화와 염증 반응을 매개하는 iNOS, COX-2 단백질의 발현 증가 역시 김 단백질을 동시투여함으로써 대조군 수준으로 회복되어졌다.

김 단백질이 D-GalN/LPS 이외의 염증성 질환에서의 효능을 검증하기 위하여 Sprague dawley rat에 4주간 에탄올과 김 단백질을 동시 투여하는 모델을 사용하였다. 장기적인 에탄올의 섭취는 간 조직의 손상을 유발하여 혈청내 GOT, GPT 수치를 증가시켰으며, 동반되어진 산화적인 스트레스로 인하여 항산화효소인 CAT, GSH, GSH-px 효소의 활성을 감소시켰으나 김 단백질을 동시투여한 군에서는 간 조직의 손상과 CAT, GSH, GSH-px 항산화효소의 활성을 회복시켜주는 것으로 나타났다. 장기적인 에탄올 섭취로 인해 활성화된 MAPK 단백질과 CYP2E1, iNOS, COX-2 단백질 발현 증가 역시, 김 단백질을 동시 투여함으로써 대조군 수준으로 회복되어지는 것으로 확인되었다. 지금까지의 결과를 보았을 때, 김 단백질은 STAT3, STAT6 전사인자를 활성화하여 염증성 M1 대식세포활성을 항염증성 성격을 가진 M2 활성으로 전환시켜 주며, D-GalN/LPS로 유발되어지는 간 질환에서 MAPK활성의 저해와 Nrf2 전사인자의 활성 촉진 및 항산화효소의 활성을 촉진시킴으로써 보호효과를 가지는 것으로 확인되었다. 또한, 장기적인 에탄올 섭취에 의한 간 손상에서도 MAPK 활성 저해와 항산화효소 활성을 촉진시킴으로써 보호효과를 가지는 것으로 나타났다.

Ⅰ. INTRODUCTION

Seaweeds mostly exist in shallow coast, but also can be found in various natural environment including deep sea areas. There is a great variety of seaweeds species been reported, for example in Korea 750 species seaweed have been reported and 1,000,000 tons (wet wt.) produced in 2012 (Lee and Gang, 1986; FAO, 2012). It has been used for a variety such as food material, medicinal material, and herbalism especially in Asia. Isolating chemical compounds from seaweeds are using various categories such as food industry, animal feed, textiles, and medication. In particular, we have to focus on therapeutic property. It has been used for folk medicine in several countries, but the scientific research began to around the 1970s (Pal *et al*., 2014).

In modern days, various biological functions of seaweed have reported. Polysaccharides are major content of seaweed such as agar, carrageenan, xylan, floridean starch, porphyran, and fucoidan (Chandini *et al*., 2008). Carrageenan have anti-tumor, anti-viral, anti-coagulant, and immunomodulation properties (Sen *et al*., 1994; Schaeffer and Krylov, 2000; Zhou *et al*., 2004; Yu *et al*., 2014). Fucoidans have been known for diverse activities such as anti-viral, anti-cancer, and anti-coagulant (Lee *et al*., 2004; Trinchero *et al*., 2009; Ermakova *et al*., 2011). Brown seaweeds have high concentration of phenol as compared to green and red seaweeds (Holdt and Kraan, 2011). Phenolic compounds from seaweeds have also known for anti-biotic, anti-bacterial, and anti fungal activity (Chandini *et al*., 2008;

Lincoln *et al*., 1991). Seaweed contains various protein content and protein kinds by species (Stengel *et al*., 2011). There are α-Kainic acid and Khalalides protein as can be obtained from seaweed. α-Kainic acid was reported potent neurophysiological activity (Ferkany and Coyle, 1983). Khalalides was reported on anti-tuberculosis and anti-bacterial activity (Bourel-Bonnet *et al*., 2005; El Sayed *et al*., 2000). Laver (*P. yezoensis*, Rhodophyta, Bangiaceae) is widely used as food in Korea, China, and Japan. *P. yezoensis* had been used as a medicine to treat emesis, diarrhea, and hemorrhoids in Oriental medicine (Kim *et al*., 2015). Production of *P. yezoensis* in Korea accounted for 34% (35 million tons) of the total production of algae (Korea Statistical Information service, 2013). The *P. yezoensis* is containing 34.3-50.2% of carbohydrates and 33.9-49% of protein (Cho *et al*., 1995). Protein makes up a large portion of *P. yezoensis* constituents and contains the essential amino acids such as threonine, tryptophan, and methionine (Dawczynski *et al*., 2007). *P. yezoensis* extraction using water or organosolvent has reported anti-microbial (Park *et al*., 2010), anti-cancer (Kim *et al*., 2015), and anti-oxidative effect (Kwak *et al*., 2005). Porphyran derived from the *P. yezoensis* has reported reducing cholesterol in the blood, anti-oxidative effect, and anti-tumor (Lee *et al*., 2010; Zhang *et al*., 2004; Yoshizawa *et al*., 1995; Osumi *et al*., 1998). *P. yezoensis* protein has reported angiotensin I converting enzyme inhibitory activities (Kim *et al*., 2005), anti-inflammation (Shin *et al*., 2011), liver protective effect against acetaminophen (Hwang *et al*., 2008). Futhermore, *P. yezoensis* lipid is containing n-3 fatty acid which has the effect of atherosclerosis prevention activities (Noda H, 1993). Although the protective

effect on the liver toxicity against acetaminophen, carbon tetrachloride, and anti-inflammatory effect at present, it was not exist liver protective activity mechanism study against ethanol and D-GalN/LPS. In particular, macrophage is directly and indirectly influence on disease progression while chemotoxicity accompanied oxidative stress and immune response. Therefore, we aimed prevention of chemotoxicity and influence on macrophage phenotype by *P. yezoensis* glycoprotein.

M1 and M2 polarization of macrophage

Macrophages are well-known not only as major regulators of innate and adaptive immunity but also important mediators of systemic metabolism, hematopoiesis, vasculogenesis, apoptosis, malignancy, and reproduction (Tugal *et al*., 2013; Lin *et al*., 2010; Nikolic-Paterson and Atkins, 2001; Aliprantis *et al*., 1996). There are two differentiation patterns, M1 and M2. M1 macrophage (classically activated macrophage) acts as regulator in host defense system. They protect from infection of bacteria, protozoa and virus. M2 macrophage (alternatively activated macrophage) has been reported on anti-inflammatory activity and important in wound healing (Barros *et al*., 2013). This plasticity can change according to macrophages environment.

M1 activation is induced by IFN-γ and LPS. M1 phenotype upregulates pro-inflammatory cytokines and chemokines (e.g. TNF-α, IL-12, IL-6, IL-1β, and CCL2), in addition, it promotes the production of ROS and RNS (Gordon and martinez, 2003; Martinez *et al*., 2009). LPS is well-known as a stimulant for macrophage study, and it is recognized for activation of TLR4-related signaling pathway. TLR4 activate MyD88 and MaL/Tirap

pathway, moreover, quickly switches to M1 phenotype. Secretion of cytokines and chemokine is related with various transcription factor such as NF-κB, AP-1, IRFs, and STAT1 (Hu and Ivashkiv, 2009). M1 macrophage has been reported to be important in chronic inflammatory diseases. Consequently, abnormal or long-term activation must be controlled to prevent damage to host.

M2 activation is related to Th2-produced IL-4 and IL-13. M2 activation is also related to both Th2-produced IL-4 and IL-13. M2 macrophage is shown that upregulation of galactose receptor, mannose receptor-1, Ym1, FIZZ1, and arginase-1 (Mantovani *et al*., 2009). Different metabolism is induced between M1 and M2. In particular, L-arginine metabolizes to produce NO in M1 macrophage but in M2 macrophage L-arginine to polyamines (Tugal *et al*., 2013).

In vitro hepatoprotective property

P. yezoensis is red algae found in Korea, China, and on the Japanese coast. In this study, we used protein extracted from this species for experiments.

Liver disease is a common health problem with numerous causes, including chemical exposure, alcohol, lipid peroxidative products, and viral infections (Hwang *et al*., 2005). Many medications have been investigated to treat liver diseases.

D-galactosamine (D-GalN) is well known *in vitro* and *in vivo* hepatic injury model. This chemical induces the loss of uridine 5'-triphosphate, uridine 5'-diphosphate, and uridine 5'-monophosphate, moreover inhibits

RNA and protein synthesis (Mato *et al*., 1999). In addition, D-GalN-induced oxidative stress is generated through reactive hydroxyl radical damage to the cell membrane via the stimulation of lipid peroxidation (MacDonald *et al*., 1987). Several studies have shown that D-GalN-induced hepatocyte death is mediated through mitogen-activated protein kinase (MAPK) and nuclear factor erythroid 2-related factor 2 (Nrf2).

Nrf2 is a transcription factor that targets genes including nicotinamide adenine dinucleotide phosphate hydrogen (NADPH), quinine oxidoreductase 1 (Nqo1), glutathione (GSH) synthesis, and glutathione-s-transferases (GST), and has many protective effects against oxidative stress. During oxidative stress, Nrf2 is translocated to the nucleus from the cytosol. As a result, antioxidant enzymes are upregulated and oxidative stress damage decreases (Sakaguch and Yokota, 1995).

MAPK include c-jun NH_2-terminal kinase (JNK), p38 MAPK, and extracellular signal-regulated kinase (ERK). These proteins are phosphorylated by D-GalN-induced oxidative stress. In particular, activated JNK induces hepatocyte death and apoptosis via activation of caspase-3 and liver cell necrosis (Hou *et al*., 2011).

Superoxide dismutase (SOD) and catalase (CAT) are important cellular defense systems that transform superoxide into oxygen and hydrogen peroxide for detoxification. Glutathione-s-transferases (GST) are a superfamily of enzymes that protect against chemical toxicity and oxidative stress (Cho *et al*., 2014; Das *et al*., 2012).

In vivo disease model

Chronic ethanol consumption induces alcoholic liver disease. It is remain to most common major causes of liver cancer and cancer death (Jemal *et al*., 2011). Ethanol generate several harmful production such as reactive oxygen species (ROS), acetaldehyde (ADH), and CYP2E1 during that metabolism (Rajendrasozhan *et al*., 2006). Generated CYP2E1 during ethanol metabolism are generative reactive products such as acetaldehyde and 1-hydroxyethyl radical (Cederbaum AI., 2010). In the ethanol consumption induced liver pathology correlates to expression of CYP2E1 level (Morgan *et al*., 2002). Although, over expression of CYP2E1 promotes lipid oxidation and oxidative stress in liver (Castillo *et al*., 1992).

ROS has been reported for protein, lipid oxidation, damage to DNA, inactivation of enzyme, and depletion of various anti-oxidative enzymes (Rouach *et al*., 1997; Fernandez-Checa *et al*., 1987; Nordmann *et al*., 1992). These results can be lead in early stage of the liver disease and dysfunction (Liu *et al*., 2005).

Glutathione (GSH), glutathione peroxidase (GSH-px), and catalase (CAT) are antioxidants, and influence anti-oxidative system (MatÉs *et al*., 1999). Enzymatic antioxidant system includes superoxide dismutase (SOD), CAT, and GSH-px (Jurczuk *et al*., 2004). Nonenzymatic antioxidants consist of glutathione, vitamine A, C, and E (Martin and Barrett, 2002). Antioxidant system can help to eliminate ROS and oxidative stress (Scott *et al*., 2000).

Recently, several studies are shown MAPK family is crucial play in cellular system such as proliferation, differentiation, development, apoptosis, and inflammatory responses (Das and Vasudevan, 2007; Venugopal *et al*., 2007; Cross *et al*., 2000; Pearson *et al*., 2001). MAPK consists of c-jun

N-terminal kinase (JNK), p38 MAP kinase, and extracellular signal-regulated kinase (ERK). Ethanol affects MAPK in a various cellular and organ systems, consequently, shows different pathologic consequences.

D-galactosamine (D-GalN) and lipopolysaccharide (LPS) are well known in hepatitis test models (Nakama *et al*., 2001). Animal models are used in hepatoprotective drug screening and to elucidate the mechanisms of clinical liver dysfunction (Chen *et al*., 2012). D-GalN induces a loss of uridine triphosphate via the galactose pathway. It inhibits RNA and protein synthesis (Wang, Y. *et al*., 2014). Subsequently, hepatic necrosis and apoptosis occur via metabolic changes (Wilhelm *et al*., 2009). LPS activates liver macrophages, which secrete diverse proinflammatory cytokines, inducing hepatic necrosis and reducing antioxidant enzymes (Jeong *et al*., 2009).

The D-GalN/LPS hepatotoxic model induces inflammatory reactions and oxidative stress in liver tissues (Jin *et al*., 2014; Wei *et al*., 2014). This occurs when inflammation and the expressions of inducible nitric oxide synthase (iNOS) and cyclooxygenase-2 (COX-2) proteins are increased (Huang *et al*., 2013). iNOS protein plays an important role in drug-induced liver injury (Wen *et al*., 2007), and COX-2 plays an important role in D-GalN/LPS-induced inflammation (Liong *et al*., 2012). Inflammation leads to the production of reactive oxygen species (ROS) such as H_2O_2, O_2^-, and OH^- (Jaechke H, 2000). ROS attacks polyunsaturated fatty acids in the cell membrane via lipid oxidation and triggers a number of pathological states, including oxidative stress (Jaeschke H, 2011).

Purpose of this study

Recently, many role of macrophage phenotype research is to be active in diabetes, obesity, cancer, and liver injury. There is in an attempt to suppression of disease progression and symptom using control of phenotypic polarization of macrophage. There does not exist as medicine related macrophage phenotype up to the present time. Some kind of cytokine proposed possibility as medicine in specific disease. *P. yezoensis* was reported diversity biological activity. We focused in anti-inflammation and chemoprotective effect. These biological activity are similar M2 phenotype macrophage function such as wound healing and anti-inflammation. Thus, we supposed *P. yezoensis* effect on macrophage phenotype and we studied influence of *P. yezoensis* glycoprotein in switch of macrophage phenotype and protective mechanism in liver injury.

Ⅱ. MATERIALS AND METHODS

1. Preparation of *Pyropia yezoensis* glycoprotein

P. yezoensis was purchased in 2013 in the Republic of Korea (Shuyup, Busan, Korea). *P. yezoensis* powder (40 g) was suspended in distilled water and stirred for 4 h at room temperature. The suspension was centrifuged at 3,000 x g at 4˚C for 10 min and vacuum filtered, followed by the addition of triple volumes (total quantity of filtrate x 3) of ethanol. Following 24 h, the solution was filtered and concentrated using rotary evaporation at 40˚C. Supernatant was added to 80% ammonium sulfate and stirred for 24 h at 4˚ C. Salt composition was then removed through a MW 3,500 Da Spectra/Por membrane (Spectrum Labs, Rancho Dominguez, CA, USA) for 48 h at 4˚C. The resulting solution was dialyzed against distilled water and then concentrated. The concentrated solution was distributed into 1.5 mL tube and freezing dried to produce a powder. It was stored at –70˚C until use, and named PYGP (Fig. 1).

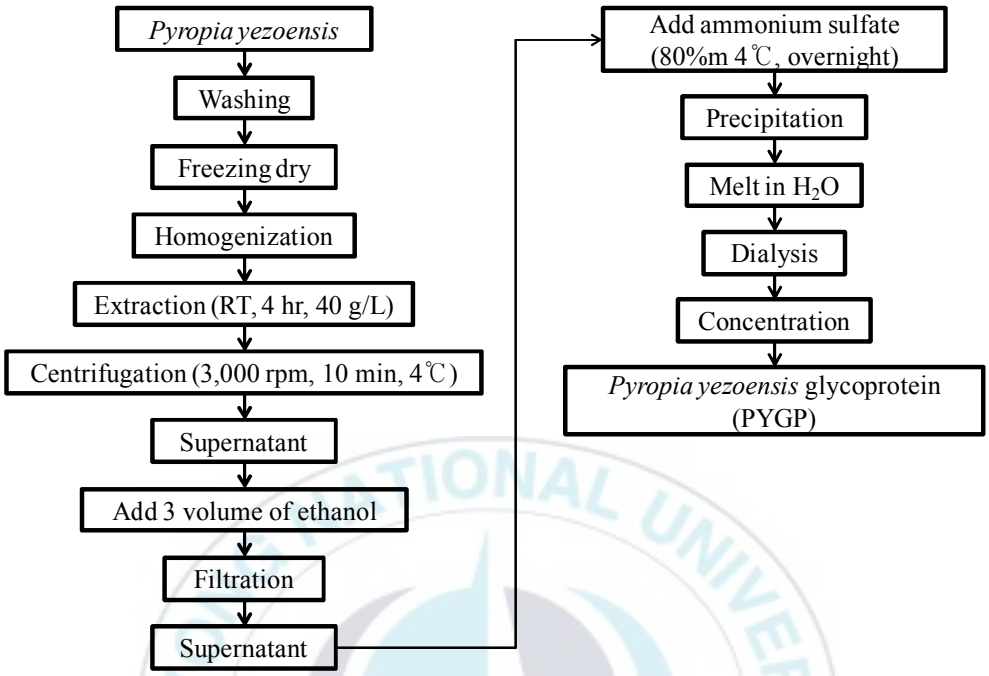

Figure 1. Preparation of *Pyropia yezoensis* glycoprotein (PYGP).

2. *In vitro* assay

2.1 Cell culture

Mouse hepatoma cells (Hepa 1c1c7) were obtained from Korean Cell Line Bank (KCLB; Seoul, Korea), human hepatocellular carcinoma cells (HepG2), human HeLa contaminant liver cells (Chang), and mouse macrophage cells (RAW 264.7) were obtained from American Type Culture Collection (ATCC; Manassas, VA, USA). Hepa 1c1c7 cells were grown in Roswell Park Memorial Institute medium 1640 (RPMI-1640). HepG2 and Chang cells were grown in Eagle's Minimum Essential Medium (MEM) and RAW 264.7 cells were grown in Dulbecco's Modified Eagle's Medium (DMEM). Every medium contained 10% fetal bovine serum (FBS; Gibco- BRL, Gaitherberg, MD, USA) and 1% penicillin/streptomycin (Gibco-BRL). Every cells were maintained at 37˚C in 5% CO_2 humidified atmosphere, sub-cultured at about 70-80% confluence in 100 mm diameter culture dish and the medium was replaced every two days.

2.2 Alteration of M1/M2 macrophage polarization by *Pyropia yezoensis* glycoprotein

2.2.1 Cell proliferation

RAW 264.7 cell proliferation was measured using a CellTiter 96 aqueous non-radioactivity cell proliferation assay (Promega). This assay determines cell proliferation based on the cleavage of 3-(4,5-dimethylthiazol-2-yl)-5-(3-carboxymethoxy-phenyl)-2-(4-sulfonyl)-2H-tetra

zolium (MTS) into a formazan product, which is soluble in tissue culture medium. RAW 264.7 cells were seeded onto 96-well plates at a density of $10x10^3$ cells/well in 100 μL medium. Cells were cultured for 24 h, following which the medium was replaced with serum-free medium (SFM) containing PYGP (20 or 40 μg/mL) for 24 h. PYGP-treated cells were then exposed to 1 μg/mL lipopolysaccharide (LPS; Sigma-Aldrich) with PYGP (20 or 40 μg/mL) for 24 h. Subsequently, cells were incubated in MTS solution for 30 min at 37˚C. Cell proliferation was measured at 490 nm using a Benchmark Plus 10730 microplate reader (Benchmark; Bio-Rad Laboratories). Percentage of cell viability was calculated by following expressions. Percentage of cell viability (%) = A_T / A_C × 100 where A_C is absorbance of control and A_T is absorbance of test group.

2.2.2 Determination of nitrite concentration

Nitrite concentration in the cultured medium was determined using Griess reagent (Enzo Life Sciences, Farmingdale, NY, USA). 50 μL of supernatant from the 96-well plates was mixed with the same volume of Griess reagent. After 30 min, absorbance was measured at 540 nm using a Benchmark Plus 10730 microplate reader (Benchmark; Bio-Rad Laboratories). Percentage of nitrite concentration was calculated by following expressions. Percentage of NO (%) = A_T / A_C × 100 where A_C is absorbance of control and A_T is absorbance of test group.

2.2.3 Determination of prostaglandin E_2

The levels of PGE_2 in the RAW 264.7 were measured using the

prostaglandin E_2 express EIA kit according to the manufacturer's instructions (Cayman, Ann Arbor, MI, USA). The absorbance was measured using a microplate reader (Benchmark plus 10730; Bio-Rad Laboratories Inc.). Percentage of prostaglandin E_2 was calculated by following expressions. Percentage of PGE_2 (%) = A_T / A_C × 100 where A_C is absorbance of control and A_T is absorbance of test group.

2.2.4 Determination of ROS generation

Intracellular levels of ROS was determined using 2',7'-dichlorofluorescenin diacetate (DCF-DA; Sigma Aldrich). RAW 264.7 cells were plated on 6-well plate and it replaced with SFM medium containing PYGP (20 or 40 μg/mL) for 24 h. PYGP-treated cells were then exposed to 1 μg/mL lipopolysaccharide (LPS; Sigma-Aldrich) with PYGP (20 or 40 μg/mL) for 24 h. The treated cells were incubated with DCF-DA for 30 min in dark. Cells were the washing twice with ice-cold PBS. Level of ROS was analyzed at an excitation wave length of 480 nm and an emission wave length of 535 nm by fluorescence microplate reader. Percentage of ROS was calculated by following expressions. Percentage of ROS (%) = A_T / A_C × 100 where A_C is absorbance of control and A_T is absorbance of test group.

2.2.5 Determination of TBARS and antioxidant enzyme

The activities of TBARS and antioxidative enzymes including superoxide dismutase (SOD), catalase (CAT), and glutathione peroxidase (GSH-px) in the RAW 264.7 cells were measured using the respective kits according to the manufacturer's instructions (TBARS assay kit; Cell Biolabs, San Diego,

CA, USA, catalase assay kit, glutathione assay kit, and glutathione s-transferase assay kit; all from Cayman, Ann Arbor, MI, USA). The absorbance was measured using a microplate reader (Benchmark plus 10730; Bio-Rad Laboratories Inc.). Percentage of TBARS and antioxidant activity was calculated by following expressions. Percentage of TBARS (%) or SOD (%) or CAT (%) or GSH-px (%) = A_T / A_C × 100 where A_C is absorbance of control and A_T is absorbance of test group.

2.2.6 Western blot analysis

RAW 264.7 cells plated onto 100 mm dishes. cells were cultured until they reached 70-80% confluence and were then pre-treated with PYGP (20 or 40 μg/mL) for 24 h. Cells were then exposed to LPS (1 μg/mL) with PYGP (20 or 40 μg/mL) for 24 h. Cells were washed with ice-cold phosphate-buffered saline (PBS; 0.15 M sodium phosphate, 0.15 M sodium chloride, pH 7.4; Gibco-BRL), following which lysis buffer (150 mM sodium chloride, 50 mM Tris-HCl [pH 7.5], 0.5% sodium deoxycholate, 0.1% sodium dodecyl sulfate, 1% triton X-100, and 2 mM ethylenediaminetetra-acetic acid) (Intron Biotechnology) with inhibitors (1 mM Na_3VO_4, 1 μg/mL aprotinin, 1 μg/mL leupeptin, 1 μg/mL pepstatin A, and 1 mM PMSF) (Sigma-Aldrich). Protein levels were determined using the bichinchominic acid assay kit (Pierce Biotechnology). Proteins were separated via 10–15% SDS-PAGE and transferred to a polyvinylidene fluoride membrane (Millipore). The transferred membrane was blocked with 1% bovine serum albumin (BSA) in TBS-T (10 mM Tris-HCl [pH 7.5], 150 mM NaCl, and 0.1% Tween 20) (USB) followed by incubation with primary

antibodies of rabbit anti-mouse STAT3 IgG polyclonal antibody (diluted 1:1,000 with BSA/TBS-T, incubated 4 h, RT), goat anti-mouse p-STAT3 IgG polyclonal antibody (diluted 1:1,000 with BSA/TBS-T, incubated 4 h, RT), rabbit anti-mouse STAT6 IgG polyclonal antibody (diluted 1:1,000 with BSA/TBS-T, incubated 4 h, RT), rabbit anti-mouse p-STAT6 IgG polyclonal antibody (diluted 1:1,000 with BSA/TBS-T, incubated 4 h, RT), rabbit anti-mouse CD163 IgG polyclonal antibody (diluted 1:1,000 with BSA/TBS-T, incubated 4 h, RT), rabbit anti-mouse CD206 IgG polyclonal antibody (diluted 1:1,000 with BSA/TBS-T, incubated 4 h, RT), rabbit anti-mouse GAPDH IgG polyclonal antibody (diluted 1:1,000 with BSA/TBS-T, incubated 4 h, RT) from Santa Cruz Biotechnology. The secondary antibodies were peroxidase-conjugated goat, mouse, and rabbit antibodies (1:10,000) from GE Healthcare Bio-Sciences. Antibody binding was visualized using the Super Signal West Pico Stable Peroxide Solution and the Super Signal West Pico Luminol/Enhancer solution (Thermo Fisher Scientific). The signal was monitored using X-ray film (Kodak) and a developer and fixer twin pack (Kodak).

2.2.7 Reverse transcription-polymerase chain reaction

RAW 264.7 cells were plated on 6-well plate and replaced with SFM medium containing PYGP (20 or 40 μg/mL) for 24 h. PYGP-treated cells were then exposed to 1 μg/mL LPS (Sigma-Aldrich) with PYGP (20 or 40 μg/mL) for 24 h. Total RNA was extracted from the cells using trizol reagent (Invitrogen, Carlsbad, CA, USA). cDNA was sythesized using RevoScript™ RT preMix (Intron Biotechnology Inc., Seongnam, Korea). The

synthesized cDNA and primer was added to 2X TOPsimple^{TM} DyeMIX-nTaq (Enzynomics Inc., Deajeon, Korea). Amplifications were performed using TOPreal™ qPCR 2X PreMIX SYBR Green (Enzynomics Inc.) in a Eco™ Real-Time PCR system (Illumina Inc., San Diego, CA, USA). Gene expression levels were normalized to GAPDH and calculated using the comparative $\Delta\Delta C_T$ method (Livak and Schmittgen, 2001). The oligonucleotide primers used for the PCR were as follows: IL-12 F-CGT GCT CAT GGC TGG TGC AAA; IL-12 R-CTT CAT CTG CAA GTT CTT GGG; IFN-γ F-ACA CTC ATT GAA AGC CTA GAA AGT CTG; IFN-γ R-ATT CTT CTT ATT GGC ACA CTC TCT ACC; IL-6 F-GTT CTC TGG GAA ATC GTG GA; IL-6 R-TGT ACT CCA GGT AGC TAT GG; NOS-2 F-CTG CAT GGA ACA GTA TAA GGC AAA C; NOS-2 R-CAG ACA GTT TCT GGT CGA TGT CAT GA; TNF-α F-AAA ATT CGA GTG ACA AGC CTG TAG; TNF-α R-CCC TTG AAG AGA ACC TGG GAG TAG; SOCS3 F-CCC GCG GGC ACC TTT CTT ATC; SOCS3 R-TCC AGG TGG CCG TTG ACA GT; IL-1β F-GTG TGG ATC CCA AGC AAT ACC CA; IL-1β R-CCA GCC CAT ACT TTA GGA AGA CAC AGA; Ym1 F-GGA TGG CTA CAC TGG AGA AA; Ym1 R-AGA AGG GTC ACT CAG GAT AA; FIZZ1 F-CCC TCC ACT GTA ACG AAG; FIZZ1 R-GTG GTC CAG TCA ACG AGT AA; ARG1 F-CTC CAA GCC AAA GTC CTT AGA G; ARG1 R-AGG AGC TGT CAT TAG GGA CAT C; IL-10 F-CTG CTC CAC TGC CTT GCT CTT ATT; IL-10 R-GTG AAG ACT TTC TTT CAA ACA AAG; STAT3 F-TGG TGT CCA GTT TAC CAC GA; STAT3 R-TGG CGG CTT AGT GAA GAA GT; Klf4 F-GCA CAC CTG CGA ACT CAC AC; Klf4 R-CCG TCC CAG TCA

CAG TGG TAA; PPARγ F-ACC ACT CGC ATT CCT TTG AC; PPARγ R-AAC CAT TGG GTC AGC TCT TG; GAPDH F-ACT CCA CTC ACG GCA AAT TCA; GAPDH R-CGC TCC TGG AAG ATG GTG AT

2.2.8 Small interference RNA transfection

Signal transducers and activators of transcription 3 (STAT3; 5′-CCC GCC AAC AAA UUA AGA ATT-3′; 3′-UUC UUA AUU UGU UGG CGG GTT-5′), STAT6 (5′-CCA AGA CAA CAA CGC CAA ATT-3′; 3′-UUU GGC GUU GUU GUC UUG GTT-5′) and silencer negative control siRNAs were purchase from GenePharma (Shanghai, China). RAW 264.7 cells were transiently transfected with siRNA for 24 h using Lipofectamine 2000 reagent (Invitrogen), according to the manufacturer's instructions. After transfection, replaced fresh culture media.

2.2.9 Proteome profiler antibody arrays assay

For analyzing the expression profiles of cytokine-related proteins, we used the Mouse Cytokine Array Kit (R&D systems Inc., MN, USA). RAW 264.7 cells were plated onto 100 mm dishes. Cells were cultured to 60-80% confluency and replaced SFM. After 6 h, medium replaced SFM with PYGP (20, 40 μg/mL). After 4 h, We treated 1 μg/mL LPS other than the control group for 20 h. The cell washed with ice-cold phosphate buffered saline (PBS) and then added 1 mL lysis buffer [1% Igepal CA-360, 20 mM Tris-Hcl (pH 8.0), 137 mM NaCl, 10% glycerol, 2 mM EDTA, 10 μg/mL aprotinin, 10 μg/mL leupeptin, 10 μg/mL pepstatin] each plate. The extracts were centrifuged at 12,000 g for 5 min and the supernatant was used. The

supernatant were analyzed by array kit according to the manufacturer's protocol.

2.3 Protective effect of PYGP on D-GalN-induced cytotoxicity in Hepa 1c1c7 cells

2.3.1 Cell proliferation

Hepa 1c1c7 cell proliferation was measured using a CellTiter 96 aqueous non-radioactivity cell proliferation assay (Promega, Madison, WI, USA). This assay determines cell proliferation based on the cleavage of 3-(4,5-dimethylthiazol-2-yl)-5-(3-carboxymethoxy-phenyl)-2-(4-sulfonyl)-2H-tetra zolium (MTS) into a formazan product, which is soluble in tissue culture medium. Hepa 1c1c7 cells were seeded onto 96-well plates at a density of $1.5x10^3$ cells/well in 100 μL medium. Cells were cultured for 24 h, following which the medium was replaced with serum-free medium (SFM) containing PYGP (20 or 40 μg/mL) for 24 h. PYGP-treated cells were then exposed to 20 mM D-galactosamine (D-GalN; Sigma-Aldrich, St. Louis, MO, USA) with PYGP (20 or 40 μg/mL) for 24 h. Subsequently, cells were incubated in MTS solution for 30 min at 37°C. Cell proliferation was measured at 490 nm using a Benchmark Plus 10730 microplate reader (Benchmark; Bio-Rad Laboratories, Hercules, CA, USA). Percentage of cell viability was calculated by following expressions. Percentage of cell viability (%) = A_T / A_C × 100 where A_C is absorbance of control and A_T is absorbance of test group.

2.3.2 Determination of lactate dehydrogenase release

Hepa 1c1c7 cell injury was quantitatively assessed via determination of lactate dehydrogenase (LDH), which is released from damaged or destroyed cells. Hepa 1c1c7 cells were seeded onto 96-well plates at a density of $1.5x10^3$ cells/well in 100 μL medium. Cells were cultured for 24 h, following which the SFM was replaced with PYGP (20 or 40 μg/mL) for 24 h. Hepa 1c1c7 cells were then exposed to either 20 mM D-GalN with PYGP (20 or 40 μg/mL) for 24 h. LDH release was measured using an LDH cytotoxicity assay kit according to the manufacturer's instructions (Cayman Chemical, Ann Arbor, MI, USA). Absorbance was then measured at 490 nm using a Benchmark Plus 10730 microplate reader (Bio-Rad Laboratories). Percentage of LDH release was calculated by following expressions. Percentage of LDH (%) = A_T / A_C × 100 where A_C is absorbance of control and A_T is absorbance of test group.

2.3.3 Determination of lipid peroxidation

Cells were collected in lysis buffer (phosphate-buffered saline, 0.05% butyl hydroxyl toluene; Cell Biolabs, San Diego, CA, USA) and homogenized on ice using a thiobarbituric acid reactive substances (TBARS) assay kit (Cell Biolabs) according to the manufacturer's instructions. Absorbance was then measured at 532 nm using a Benchmark Plus 10730 microplate reader (Bio-Rad Laboratories). Percentage of lipid peroxidation was calculated by following expressions. Percentage of TBARS (%) = A_T / A_C × 100 where A_C is absorbance of control and A_T is absorbance of test group.

2.3.4 Determination of antioxidant enzyme

SOD (Superoxide dismutase assay kit; Cayman Chemical Co., Ann Arbor, MI, USA), CAT (Catalase assay kit; Cayman Chemical Co.), and GST (Glutathione s-transferase assay kit; Cayman Chemical Co.) activities of Hepa 1c1c7 cells were measured according to the manufacturer's instructions. Absorbance was then measured using a Benchmark microplate reader (Benchmark Plus 10730; Bio-Rad Laboratories, Inc.). Percentage of antioxidant activity was calculated by following expressions. Percentage of SOD (%) or CAT (%) or GST (%) = A_T / A_C × 100 where A_C is absorbance of control and A_T is absorbance of test group.

2.3.5 Western blot analysis

Hepa 1c1c7 cells were plated onto 100 mm dishes. Cells were cultured until they reached 60-80% conflence and were then pre-treated with PYGP (20 or 40 μg/mL) for 24 h. Cells were then exposed to D-GalN (20 mM) with PYGP (20 or 40 μg/mL) for 24 h. Cells were washed with ice-cold phosphate-buffered saline (PBS; 0.15 M sodium phosphate, 0.15 M sodium chloride, pH 7.4; Gibco-BRL), following which lysis buffer [20 mM Tris-base (pH 7.5), 150 mM NaCl, 0.25% Na-deoxycholate, 1 mM EDTA, 1 mM ethylene glycol tetraacetic acid, 1% Triton X-100 from iNtRON Biotechnology, Seoul, Korea; containing 2.5 M sodium pyrophosphate, 1 mM β-glycerophosphate, 1 mM Na_3VO_4, 1 μg/mL aprotinin, 1 μg/mL leupeptin, 1 μg/mL pepstatin A and 1 mM phenylmethylsulfonyl floride from Sigma-Aldrich] was added. Protein content was determined using a

bicinchoninic acid protein assay kit (Pierce Biotechnology, Inc., Rockford, IL, USA). Proteins were separated using 10-15% SDS-PAGE and then transferred to a polyvinylidene floride membrane (Millipore, Billerica, MA, USA). The transferred membrane was blocked at room temperature with 1% bovine serum albumin (BSA) in Tris-buffered saline with Tween 20 [TBS-T; 10 mM Tris-HCl (pH 7.5), 150 mM NaCl and 0.1% Tween 20] and then incubated, with agitation, with the indicated primary antibodies: Rabbit anti-mouse ERK immunoglobulin G (IgG) polyclonal antibody [diluted 1:1,000 with BSA/TBS-T; incubated for 4 h at room temperature (RT)], rabbit anti-phosphorylated (p)-ERK IgG polyclonal antibody (diluted 1:1,000 with BSA/TBS-T; incubated for 4 h at RT), mouse anti-mouse JNK IgG monoclonal antibody (diluted 1:1,000 with BSA/TBS-T; incubated for 4 h at RT), mouse anti-mouse p-JNK IgG monoclonal antibody (diluted 1:1,000 with BSA/TBS-T; incubated for 4 h at RT), rabbit anti-mouse p38 IgG polyclonal antibody (diluted 1:1,000 with BSA/TBS-T; incubated for 4 h at RT), mouse anti-mouse p-p38 IgG monoclonal antibody (diluted 1:1,000 with BSA/TBS-T; incubated for 4 h at RT), rabbit anti-mouse Nrf2 IgG polyclonal antibody (diluted 1:1,000 with BSA/TBS-T; incubated for 4 h at RT), goat anti-mouse Nqo1 IgG polyclonal antibody (diluted 1:1,000 with BSA/TBS-T; incubated for 4 h at RT), mouse anti-mouse GST IgG monoclonal antibody (diluted 1:1,000 with BSA/TBS-T; incubated for 4 h at RT), and rabbit anti-mouse heme oxygenase (HO)-1 IgG polyclonal antibody (diluted 1:1,000 with BSA/TBS-T; incubated for 4 h at RT), which were all purchased from Santa Cruz Biotechnology, Inc. (Dallas, TX, USA). The secondary antibody was a peroxidase-conjugated goat, mouse, and rabbit

antibody (1:10,000; GE Healthcare, Little Chalfont, UK). Super Signal West Pico Stable Peroxide Solution and the Super Signal West Pico Luminol/Enhancer solution (Thermo Fisher Scientifi, Rockford, IL, USA) were then added and the signal was monitored using X-ray fim (Kodak, Rochester, NY, USA) and a developer and fixer twin pack (Kodak).

2.4 Protective effect on D-GalN-induced toxicity in primary rat hepatocyte

2.4.1 Preparation of rat hepatocyte

Male Sprague dawley (6 weeks of age) was obtained from samtaco (Osan, Korea). Animal studies were carried out in accordance with the Animal Ethics Committee of the Pukyong National university (2015-01; Busan, Korea). Primary rat hepatocytes were isolated from rat liver using the collagenase perfusion method. Rats were anesthetized with zoletil (Bayer Korea, Seoul, Korea):rompun (Virbac, Carros, France) 5:2 ratio mix. After the rat was anesthetized, the liver was perfused with 1x Hank's buffered salt solution (HBSS; Gibco), without magnesium or calcium, with 0.5 mM EGTA through the portal vein to rinse the blood out. Then, liver was perfused with digestion medium (DMEM-low glucose with 1% penicillin/streptomycin, 15 mM HEPES, and 100 units/mL type IV collagenase; Gibco) begin to swell. The liver was then cut connection and immediately place the liver into the 100 mm dish containing digestion medium. After minced, the solution containing mixed cells debris was filtered through a 70 micron filter. Subsequently, the filtrate was centrifuged

at 50 x g, 2 min, 4˚C, the cells were washed with F-12 HAM's (Hycolone, Logan, UT, USA) three times and the seeded in type I collagen (Gibco) coated plate with DMEM (Gibco) containing 10% FBS, 1% penicillin/streptomycin at 37˚C in a humidified 5% CO_2 atmosphere. The cells were incubated with fresh Williams' E medium without FBS 24 h prior to the experiments.

2.4.2 Determination of lactate dehydrogenase release

Primary hepatocyte injury was quantitatively assessed via determination of lactate dehydrogenase (LDH), which is released from damaged or destroyed cells. Primary hepatocyte were seeded onto 96-well plates at a density of $2.3x10^3$ cells/well in 100 μl medium. Cells were cultured for 24 h, following which the SFM was replaced with PYGP (80 or 160 μg/mL) for 24 h. Primary hepatocyte were then exposed to either 25 mM D-GalN with PYGP (80 or 160 μg/mL) for 24 h. LDH release was measured using an LDH cytotoxicity assay kit according to the manufacturer's instructions (Cayman Chemical, Ann Arbor, MI, USA). Absorbance was then measured at 490 nm using a Benchmark Plus 10730 microplate reader (Bio-Rad Laboratories). Percentage of LDH release was calculated by following expressions. Percentage of LDH (%) = A_T / A_C × 100 where A_C is absorbance of control and A_T is absorbance of test group.

2.4.3 Western blot analysis

Primary hepatocyte was plated onto 100 mm dishes. Cells were cultured until they reached 60-80% confluence and were then pre-treated with PYGP

(80 or 160 μg/mL) for 24 h. Cells were then exposed to D-GalN (20 mM) with PYGP (20 or 40 μg/mL) for 24 h. Cells were washed with ice-cold phosphate-buffered saline (PBS; 0.15 M sodium phosphate, 0.15 M sodium chloride, pH 7.4; Gibco-BRL), following which lysis buffer [20 mM Tris-base (pH 7.5), 150 mM NaCl, 0.25% Na-deoxycholate, 1 mM EDTA, 1 mM ethylene glycol tetraacetic acid, 1% Triton X-100 from iNtRON Biotechnology, Seoul, Korea; containing 2.5 M sodium pyrophosphate, 1 mM β-glycerophosphate, 1 mM Na_3VO_4, 1 μg/mL aprotinin, 1 μg/mL leupeptin, 1 μg/mL pepstatin A, and 1 mM phenylmethylsulfonyl floride from Sigma-Aldrich] was added. Protein content was determined using a bicinchoninic acid protein assay kit (Pierce Biotechnology, Inc., Rockford, IL, USA). Proteins were separated using 10-15% SDS-PAGE and then transferred to a polyvinylidene floride membrane (Millipore, Billerica, MA, USA). The transferred membrane was blocked at room temperature with 1% bovine serum albumin (BSA) in Tris-buffered saline with Tween 20 [TBS-T; 10 mM Tris-HCl (pH 7.5), 150 mM NaCl, and 0.1% Tween 20] and then incubated, with agitation, with the indicated primary antibodies: Rabbit anti-mouse ERK immunoglobulin G (IgG) polyclonal antibody [diluted 1:1,000 with BSA/TBS-T; incubated for 4 h at room temperature (RT)], rabbit anti phosphorylated (p)-ERK IgG polyclonal antibody (diluted 1:1,000 with BSA/TBS-T; incubated for 4 h at RT), mouse anti-mouse JNK IgG monoclonal antibody (diluted 1:1,000 with BSA/TBS-T; incubated for 4 h at RT), mouse anti-mouse p-JNK IgG monoclonal antibody (diluted 1:1,000 with BSA/TBS-T; incubated for 4 h at RT), rabbit anti-mouse p38 IgG polyclonal antibody (diluted 1:1,000 with BSA/TBS-T; incubated for 4 h at

RT), mouse anti-mouse p-p38 IgG monoclonal antibody (diluted 1:1,000 with BSA/TBS-T; incubated for 4 h at RT), which were all purchased from Santa Cruz Biotechnology, Inc. (Dallas, TX, USA). The secondary antibody was a peroxidase-conjugated goat, mouse, and rabbit antibody (1:10,000; GE Healthcare, Little Chalfont, UK). Super Signal West Pico Stable Peroxide Solution and the Super Signal West Pico Luminol/Enhancer solution (Thermo Fisher Scientifi, Rockford, IL, USA) were then added and the signal was monitored using X-ray film (Kodak, Rochester, NY, USA) and a developer and fixer twin pack (Kodak).

3. *In vivo* assay

3.1 PYGP regulates antioxidant status and prevents hepatotoxicity in D-GalN/LPS-induced acute liver failure in rats

3.1.1 Experimental animals

Male Sprague-Dawley (6 weeks old) rats were purchased from Samtaco. Animal studies were carried out in accordance with the Animal Ethics Committee of the Pukyong National university (2014-02; Busan, Korea). The rats were allowed to adapt to laboratory conditions (temperature: 23 ± 3°C, 12 h light/12 h dark cycle, 50% humidity) with free access to water and food.

3.1.2 Experimental design

Animals were randomly divided into four groups of five animals each as

follows: group 1, control rats that received distilled water only; group 2, D-GalN 500 mg/kg/BW + LPS 10 μg/kg/BW; group 3: D-GalN 500 mg/kg/BW + LPS 10 μg/kg/BW + PYGP 150 mg/kg/BW; and group 4, D-GalN 500 mg/kg/BW + LPS 10 μg/kg/BW + PYGP 300 mg/kg/BW. PYGP was administered orally once a day for 7 days. Hepatotoxicity in the rats was induced by intraperitoneal injection of D-GalN/LPS (Sigma-Aldrich) at a dose of 500 mg/kg/BW D-GalN and 10 μg/kg/BW LPS. All groups were sacrificed for blood and liver collection at 6 h after hepatotoxicity induction.

3.1.3 Determination of lipid peroxidation

The liver was collected in 1x butyl hydroxyl toluene (BHT; Cell Biolabs, San Diego, CA, USA) and homogenized on ice according to the TBARS assay kit protocol (Cell Biolabs). The absorbance at 532 nm was measured using a microplate reader (Benchmark plus 10730; Bio-Rad Laboratories). Percentage of lipid peroxidation was calculated by following expressions. Percentage of TBARS (%) = A_T / A_C × 100 where A_C is absorbance of control and A_T is absorbance of test group.

3.1.4 Determination of antioxidant enzyme

The activities of antioxidative enzymes including catalase (CAT), glutathione s-transferase (GST), and level of glutathione (GSH) in the liver were measured using the respective kits according to the manufacturer's instructions (catalase assay kit, glutathione assay kit, and glutathione s-transferase assay kit; all from Cayman, Ann Arbor, MI, USA). The

absorbance was measured using a microplate reader (Benchmark plus 10730; Bio-Rad Laboratories). Percentage of antioxidant activity and level was calculated by following expressions. Percentage of CAT (%) or GSH (%) or GST (%) = A_T / A_C × 100 where A_C is absorbance of control and A_T is absorbance of test group.

3.1.5 Western blot analysis

Liver tissue protein was homogenized in lysis buffer (150 mM sodium chloride, 50 mM Tris-HCl [pH 7.5], 0.5% sodium deoxycholate, 0.1% sodium dodecyl sulfate, 1% triton X-100, and 2 mM ethylenediaminetetra-acetic acid) (Intron Biotechnology) with inhibitors (1 mM Na_3VO_4, 1 μg/mL aprotinin, 1 μg/mL leupeptin, 1 μg/mL pepstatin A, and 1 mM PMSF) (Sigma-Aldrich). Protein levels were determined using the bichinchominic acid (BCA) assay kit (Pierce Biotechnology). Proteins were separated via 10–15% SDS-PAGE and transferred to a polyvinylidene fluoride membrane (Millipore). The membrane was blocked with 1% bovine serum albumin in TBS-T (10 mM Tris-HCl [pH 7.5], 150 mM NaCl, and 0.1% Tween 20) (USB) followed by incubation with primary antibodies of rabbit anti-rat ERK IgG polyclonal antibody (diluted 1:1,000 with BSA/TBS-T, incubated 4 h, RT), rabbit anti-rat phosphorylated p-ERK IgG polyclonal antibody (diluted 1:1,000 with BSA/TBS-T, incubated 4 h, RT), mouse anti-rat JNK IgG monoclonal antibody (diluted 1:1,000 with BSA/TBS-T, incubated 4 h, RT), mouse anti-rat p-JNK IgG monoclonal antibody (diluted 1:1,000 with BSA/TBS-T, incubated 4 h, RT), rabbit anti-rat p38 IgG polyclonal antibody (diluted 1:1,000 with BSA/TBS-T,

incubated 4 h, RT), mouse anti-rat p-p38 IgG monoclonal antibody (diluted 1:1,000 with BSA/TBS-T, incubated 4 h, RT), mouse anti-rat iNOS IgG polyclonal antibody (diluted 1:1,000 with BSA/TBS-T, incubated 4 h, RT) and goat anti-rat COX-2 IgG polyclonal antibody (diluted 1:1,000 with BSA/TBS-T, incubated 4 h, RT) from Santa Cruz Biotechnology. The secondary antibodies were peroxidase-conjugated goat, mouse, and rabbit antibodies (1:10,000) from GE Healthcare Bio-Sciences. Antibody binding was visualized using the Super Signal West Pico Stable Peroxide Solution and the Super Signal West Pico Luminol/Enhancer solution (Thermo Fisher Scientific Inc.). The signal was examined using Kodak X-ray film (Kodak) and a developer and fixer twin pack (Kodak).

3.2 Protective effect of PYGP on ethanol-induced hepatotoxicity in rat

3.2.1 Experimental animals

Male Sprague-Dawley (6 weeks old) rats were purchased from Samtaco. Animal studies were carried out in accordance with the Animal Ethics Committee of the Pukyong National university (2014-02; Busan, Korea). The rats were allowed to adapt to laboratory conditions (temperature: 23 ± 3°C, 12 h light/12 h dark cycle, 50% humidity) with free access to water and food.

3.2.2 Experimental design

Animals were randomly divided into four groups of five rats each as

follows: group 1, control rats that received distilled water only (CON group); group 2, 20% ethanol 3.7 g/kg/BW (EtOH group); group 3, 20% ethanol 3.7 g/kg/BW + PYGP 150 mg/kg/BW (EtOH + 150 group); and group 4, 20% ethanol 3.7 g/kg/BW + PYGP 300 mg/kg/BW (EtOH + 300 group). PYGP and ethanol were administered orally once a day for 30 days. All groups were sacrificed for blood and liver collection at the end of experimental period (31 days after). Brood was collected immediately, Liver was frozen in liquid nitrogen and store at -70°C until use.

3.2.3 Determination of GOT and GPT

Chronic hepatic damages were measured by detecting serum GOT and GPT activities using the enzymatic analysis kit (Asan Pharmaceuticals, Hwasung, Korea) according to the manufacturer's instructions. The absorbance was measured using a UV spectrometer (Ultrospec 2100 pro; Amersham Pharmacia biotech, Cambridge, United Kingdom). Percentage of GOT and GPT level was calculated by following expressions. Percentage of GOT (%) or GPT (%) = A_T / A_C × 100 where A_C is absorbance of control and A_T is absorbance of test group.

3.2.4 Determination of antioxidant enzyme

The activities of anti-oxidative enzymes including CAT, GSH-px, and level of GSH in the liver were measured using the respective kits according to the manufacturer's instructions (catalase assay kit, glutathione assay kit, and glutathione peroxidase assay kit; all from Cayman, Ann Arbor, MI, USA). The absorbance was measured using a microplate reader (Benchmark

plus 10730; Bio-Rad Laboratories Inc.). Percentage of antioxidant activity and level was calculated by following expressions. Percentage of CAT (%) or GSH (%) or GSH-px (%) = A_T / A_C × 100 where A_C is absorbance of control and A_T is absorbance of test group.

3.2.5 Western blot analysis

Liver tissue protein was homogenized in lysis buffer (150 mM sodium chloride, 50 mM Tris-HCl [pH 7.5], 0.5% sodium deoxycholate, 0.1% sodium dodecyl sulfate, 1% triton X-100, and 2 mM ethylenediaminetetra-acetic acid) (Intron Biotechnology) with inhibitors (1 mM Na_3VO_4, 1 μg/mL aprotinin, 1 μg/mL leupeptin, 1 μg/mL pepstatin A, and 1 mM PMSF) (Sigma-Aldrich). Protein levels were determined using the bichinchominic acid assay kit (Pierce Biotechnology). Proteins were separated via 10–15% SDS-PAGE and transferred to a polyvinylidene fluoride membrane (Millipore). The transferred membrane was blocked with 1% bovine serum albumin (BSA) in TBS-T (10 mM Tris-HCl [pH 7.5], 150 mM NaCl, and 0.1% Tween 20) (USB) followed by incubation with primary antibodies of rabbit anti-rat ERK IgG polyclonal antibody (diluted 1:1,000 with BSA/TBS-T, incubated 4 h, RT), rabbit anti-rat phosphorylated p-ERK IgG polyclonal antibody (diluted 1:1,000 with BSA/TBS-T, incubated 4 h, RT), mouse anti-rat JNK IgG monoclonal antibody (diluted 1:1,000 with BSA/TBS-T, incubated 4 h, RT), mouse anti-rat p-JNK IgG monoclonal antibody (diluted 1:1,000 with BSA/TBS-T, incubated 4 h, RT), rabbit anti-rat p38 IgG polyclonal antibody (diluted 1:1,000 with BSA/TBS-T, incubated 4 h, RT), mouse anti-rat p-p38 IgG monoclonal antibody (diluted

1:1,000 with BSA/TBS-T, incubated 4 h, RT), mouse anti-rat iNOS IgG polyclonal antibody (diluted 1:1,000 with BSA/TBS-T, incubated 4 h, RT), goat anti-rat COX-2 IgG polyclonal antibody (diluted 1:1,000 with BSA/TBS-T, incubated 4 h, RT), rabbit anti-rat CYP2E1 IgG polyclonal antibody (diluted 1:1,000 with BSA/TBS-T, incubated 4 h, RT), and rabbit anti-rat GAPDH IgG polyclonal antibody (diluted 1:1,000 with BSA/TBS-T, incubated 4 h, RT) from Santa Cruz Biotechnology. The secondary antibodies were peroxidase-conjugated goat, mouse, and rabbit antibodies (1:10,000) from GE Healthcare Bio-Sciences. Antibody binding was visualized using the Super Signal West Pico Stable Peroxide Solution and the Super Signal West Pico Luminol/Enhancer solution (Thermo Fisher Scientific). The signal was monitored using X-ray film (Kodak) and a developer and fixer twin pack (Kodak).

4. Statistical analysis

Values are presented as the mean ± standard deviation and data were analyzed with SPSS ver. 10.0 software (SPSS Inc., Chicago, IL, USA) using an analysis of variance followed by a Duncan's multiple range test. P-values<0.05 was considered to indicate a statistically significant difference between values.

Ⅲ. RESULT AND DISCUSSION

1. Alteration of M1/M2 macrophage polarization by PYGP

1.1 Effect of PYGP on cell viability

Cytotoxicity of PYGP prepared with various concentrations was measured using MTS assay in RAW 264.7 cells (Fig. 2). Consequently, PYGP was not significantly influenced to the cell viability up to 40 μg/mL.

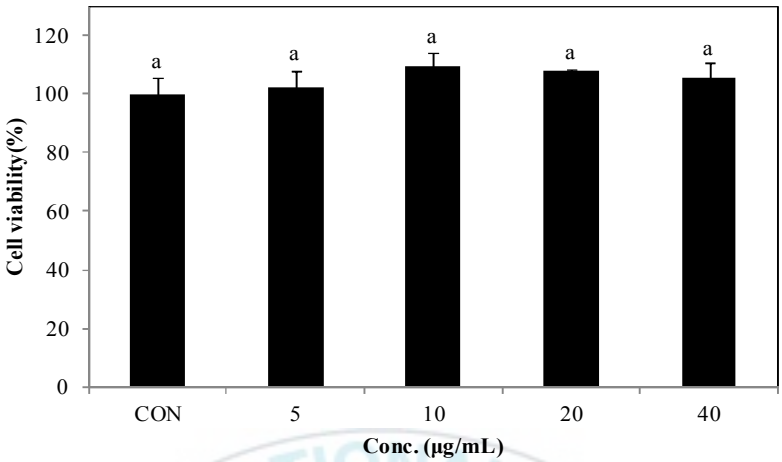

Figure 2. Cytotoxic effect of PYGP on LPS-induced inflammation in RAW 264.7 cells. Cells were pre-treated with PYGP (5, 10, 20, and 40 μg/mL) for 24 h and then treated with 1 μg/mL LPS with PYGP (5, 10, 20, and 40 μg/mL) for 24 h. Values are presented as the mean ± standard deviation. Values with different letters are significantly different ($P<0.05$).

1.2 Effect of PYGP on LPS-induced NO release

We used the Griess reagent to determine the production of NO (Fig. 3). LPS-stimulated M1 macrophages made the toxic NO, and release to the extracellular. Culture media NO concentration was high in LPS only treated group. However in the presence of PYGP, the concentration of NO in the culture media was inhibited in a dose-dependent manner.

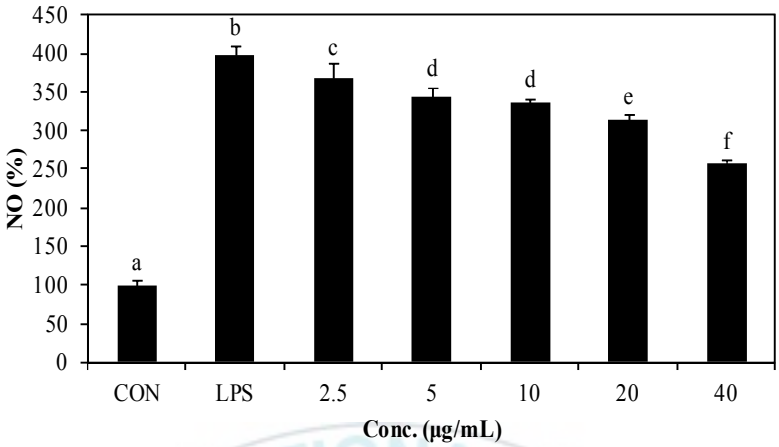

Figure 3. Effect of PYGP on the level of the NO following LPS-induced M1 activation. RAW 264.7 cells were pre-treated with PYGP (2.5, 5, 10, 20, and 40 μg/mL) for 24 h and then administered 1 μg/mL LPS with PYGP (2.5, 5, 10, 20, and 40 μg/mL) for 24 h. Values are presented as the mean ± standard deviation. Values with different letters are significantly different ($P<0.05$).

1.3 Effect of PYGP on LPS-induced PGE_2 production

The production levels of PGE_2 were measured in the LPS-activated RAW 264.7 cells (Fig. 4). PGE_2 secreted into supernatant of the cultures was estimated by PGE_2 express ELISA kit. After treatment with LPS 1 μg/mL, PGE_2 expression in the medium is remarkably advanced. However, when RAW 264.7 cells were pre-treated with PYGP, the PGE_2 expression was decreased significantly.

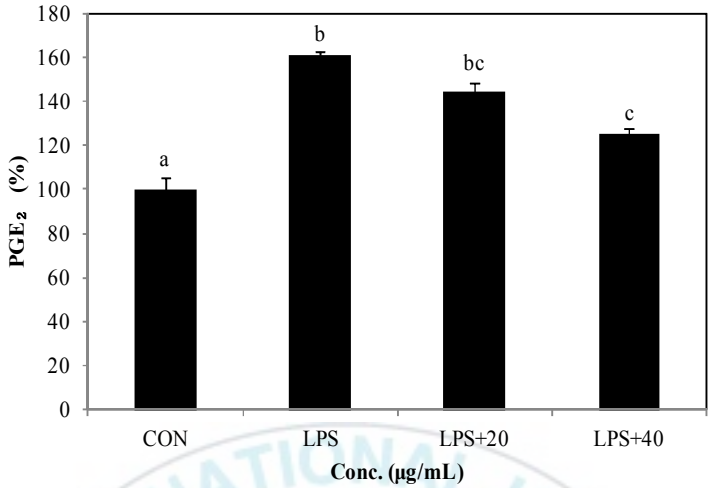

Figure 4. Effect of PYGP on the level of the PGE_2 following LPS-induced M1 activation. RAW 264.7 cells were pre-treated with PYGP (20 and 40 μg/mL) for 24 h and then administered 1 μg/mL LPS with PYGP (20 and 40 μg/mL) for 24 h. Values are presented as the mean ± standard deviation. Values with different letters are significantly different ($P<0.05$).

1.4 Effect of PYGP on LPS-induced TBARS and ROS generation

TBARS formation induces LPS-stimulated RAW 264.7 cells via oxidative stress mechanism (Fig. 5A). The results of present study revealed that TBARS levels in the cells were significantly higher in LPS-only treatment group. In addition, pre-treatment of PYGP was significantly inhibited the TBARS level of RAW 264.7 cells in comparison with the LPS-only treatment group.

We measured whether PYGP attenuated ROS generation in LPS-induced RAW 264.7 cells using DCF-DA (Fig. 5B). LPS-stimulated RAW 264.7 cells significantly generated ROS compare with CON group. However, pre-treatment with PYGP remarkably inhibited the LPS-stimulated increase in ROS generation levels.

(A)

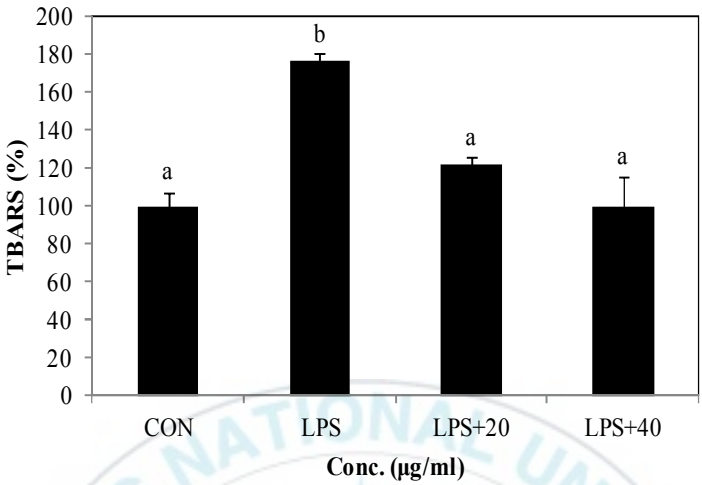

(B)

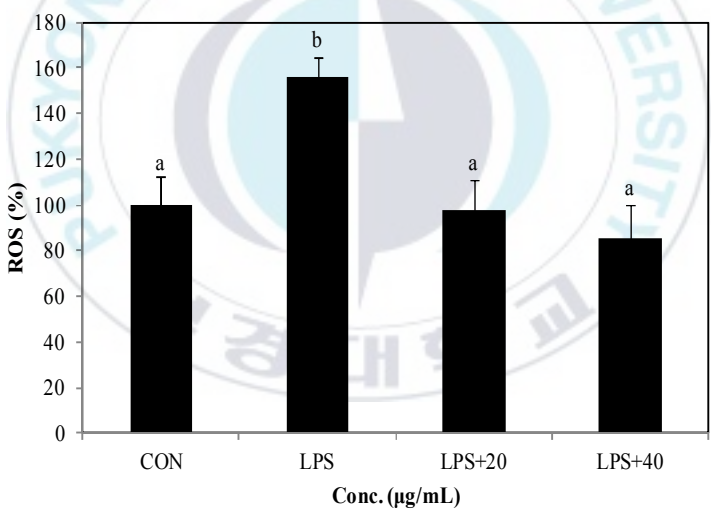

Figure 5. Effect of PYGP on the level of the TBARS and ROS following LPS-induced M1 activation. RAW 264.7 cells were pre-treated with PYGP (20 and 40 μg/mL) for 24 h and then administered 1 μg/mL LPS with PYGP (20 and 40 μg/mL) for 24 h. TBARS level (A). ROS level (B). Values are presented as the mean ± standard deviation. Values with different letters are significantly different ($P<0.05$).

1.5 Effect of PYGP on M1 polarization markers

It is known that RAW 264.7 macrophages produce pro-inflammatory cytokines in M1 phenotype. To identify the effect of PYGP to LPS-exposed RAW 264.7 cells, we observed mRNA and protein expression of the pro-inflammatory cytokine (Fig. 6, 7). The real-time PCR analysis revealed that LPS upregulate mRNA expression of the pro-inflammatory cytokine such as IL-12, IL-6, IL-1β, NOS-2, IFN-γ, and TNF-α. Pre-treatment of PYGP was significantly suppressed the expression of pro-inflammatory cytokines mRNA. These results suggest that PYGP prevent to pro-inflammatory cytokine expression and M1 activation in LPS-activated RAW 264.7 cells.

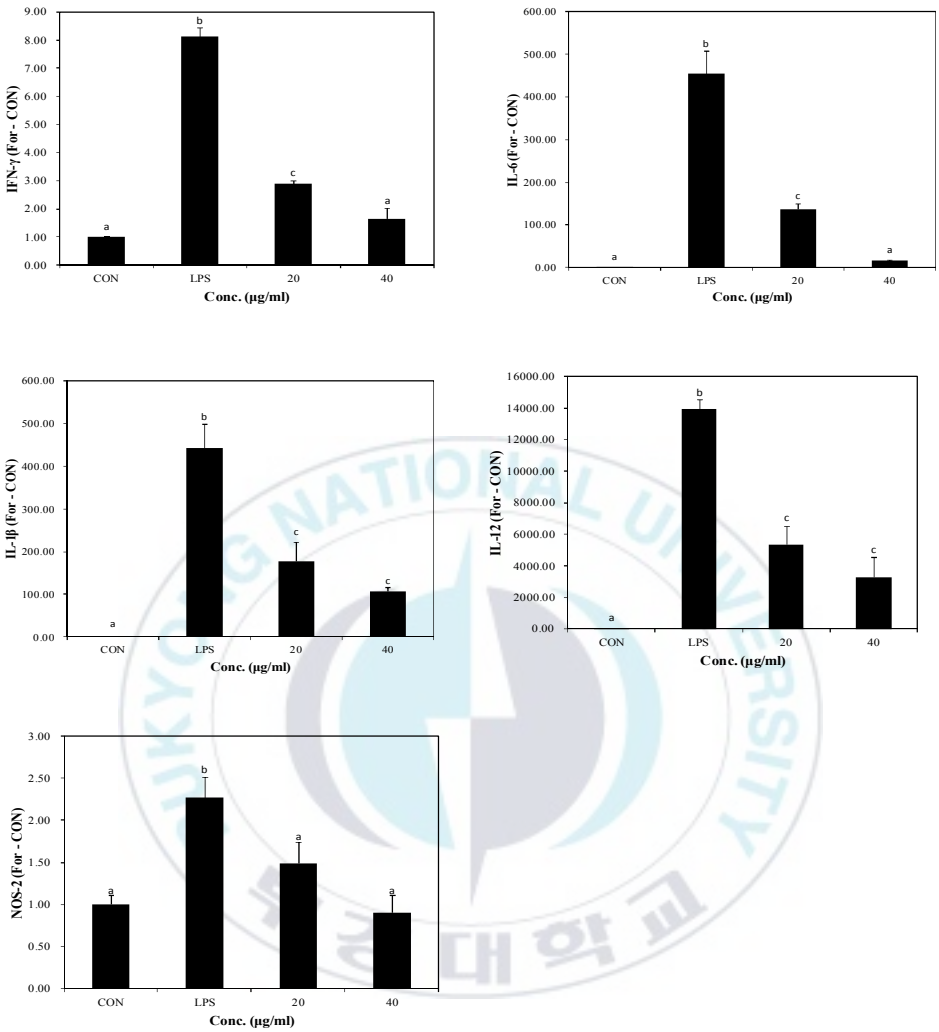

Figure 6. Effect of PYGP on the level of the M1 marker following LPS-induced M1 activation. RAW 264.7 cells were pre-treated with PYGP (20 and 40 μg/mL) for 24 h and then administered 1 μg/mL LPS with PYGP (20 and 40 μg/mL) for 24 h. Values are presented as the mean ± standard deviation. Values with different letters are significantly different ($P<0.05$).

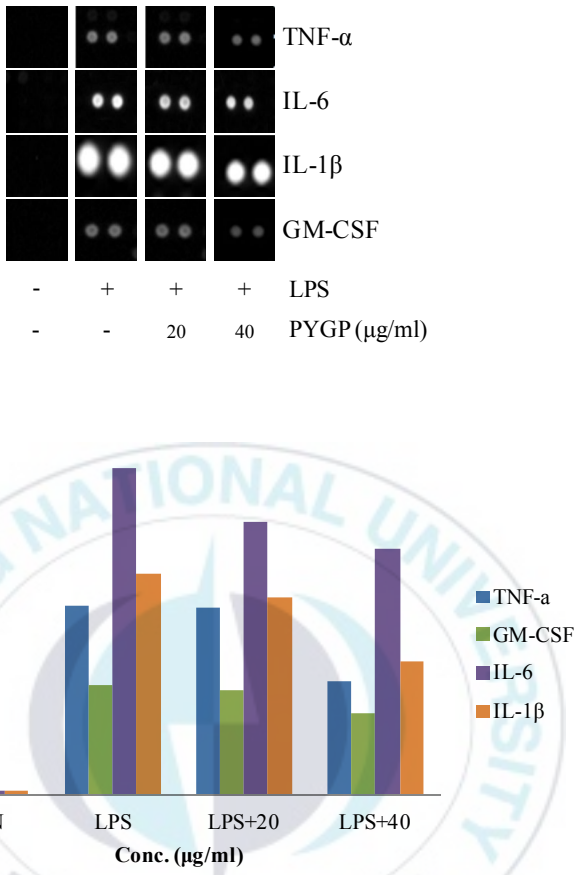

Figure 7. Effect of PYGP on the level of the cytokine following LPS-induced M1 activation. RAW 264.7 cells were pre-treated with PYGP (20 and 40 μg/mL) for 24 h and then administered 1 μg/mL LPS with PYGP (20 and 40 μg/mL) for 24 h. The expression levels of the TNF-α, G-CSF, GM-CSF, IL-6, IL-16, and IL-1β cytokine were examined by array kit. Values are presented as the mean ± standard deviation. Values with different letters are significantly different ($P<0.05$).

1.6 Effect of PYGP on M2 polarization markers

RAW 264.7 macrophage is occur alteration of metabolism in M2 polarization. Consequently, macrophage is produce Ym1, ARG1, and FIZZ1. Control group and M1 activity by the LPS treated group were not observed expression of M2 marker mRNA. However, PYGP-treated group shown that the expression of M2 marker mRNA increases (Fig. 8). These results indicate that the LPS-induced M1 activity macrophage has switch to M2 activity by PYGP.

There is observation that upregulation of several non-opsonic receptors such as CD206 and CD163 in M2 activation macrophage. We used Western blot analysis for investigation of CD206, CD163 protein expression (Fig. 9). LPS treatment was decreased CD206, CD163 in RAW 264.7 cells. In the pre-treatment of PYGP, the expression level of CD206 and CD163 were significantly increased compare with CON and LPS treated-only groups.

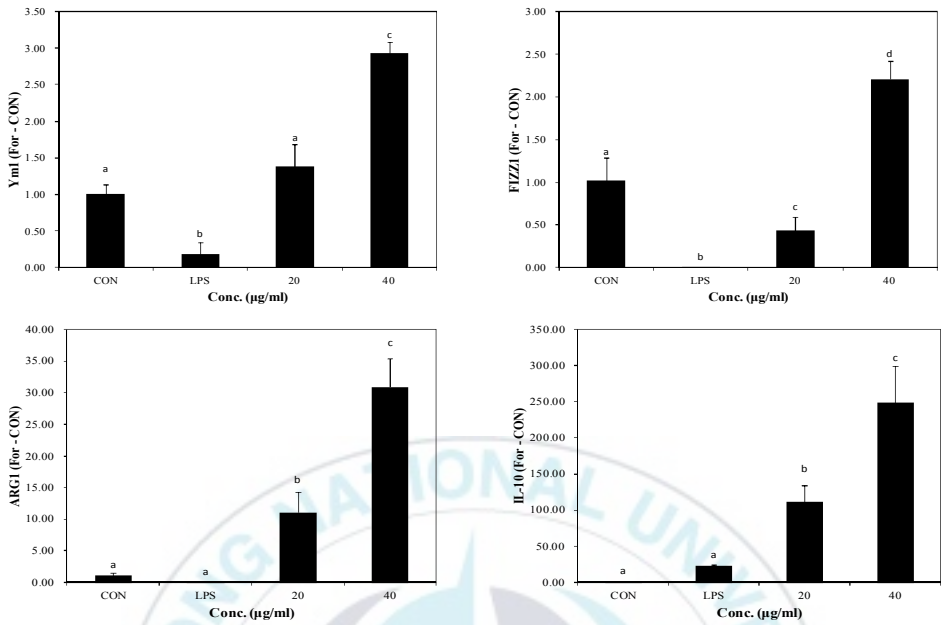

Figure 8. Effect of PYGP on the level of the M2 marker following LPS-induced M1 activation. RAW 264.7 cells were pre-treated with PYGP (20 and 40 μg/mL) for 24 h and then administered 1 μg/mL LPS with PYGP (20 and 40 μg/mL) for 24 h. Values are presented as the mean ± standard deviation. Values with different letters are significantly different ($P<0.05$).

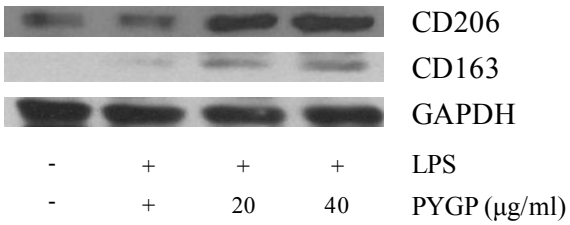

Figure 9. Effect of PYGP on the level of the CD206 and CD163 following LPS-induced M1 activation. RAW 264.7 cells were pre-treated with PYGP (20 and 40 μg/mL) for 24 h and then administered 1 μg/mL LPS with PYGP (20 and 40 μg/mL) for 24 h.

1.7 Effect of PYGP on STAT3, STAT6 signaling pathway

STAT3 and STAT6 are well known transcription factor that induces M2 activation of macrophage and inhibit pro-inflammatory effect. Thus, we measured the phosphorylation of STAT3 and STAT6 by Western blot analysis (Fig. 10). This result shown that LPS treatment was not effected on STAT3 and STAT6 phosphorylation. PYGP pre-treatment groups were dose dependently mediated reduced the phosphorylation of STAT3 and STAT6. However, total STAT3 and STAT6 protein expression levels were not altered following treatment with LPS or pre-treated PYGP.

PPARγ and KLF4 were reported increase of expression by STAT6 phosphorylation. Increased expression of PPARγ and KLF4 promote switch to M2 phenotype macrophage. We used RT-PCR to determine mRNA expression difference of PPARγ and KLF4 by LPS and PYGP treatment (Fig. 11). LPS was not effected on PPARγ and KLF4 mRNA expression compare with CON group. However PYGP pretreated groups were increased PPARγ and KLF4 mRNA expression in a dose dependent manner.

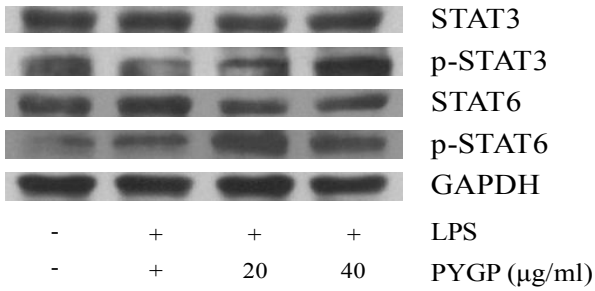

Figure 10. Effect of PYGP on the expression of the STAT3 and STAT6 following LPS-induced M1 activation. RAW 264.7 cells were pre-treated with PYGP (20 and 40 μg/mL) for 24 h and then administered 1 μg/mL LPS with PYGP (20 and 40 μg/mL) for 24 h.

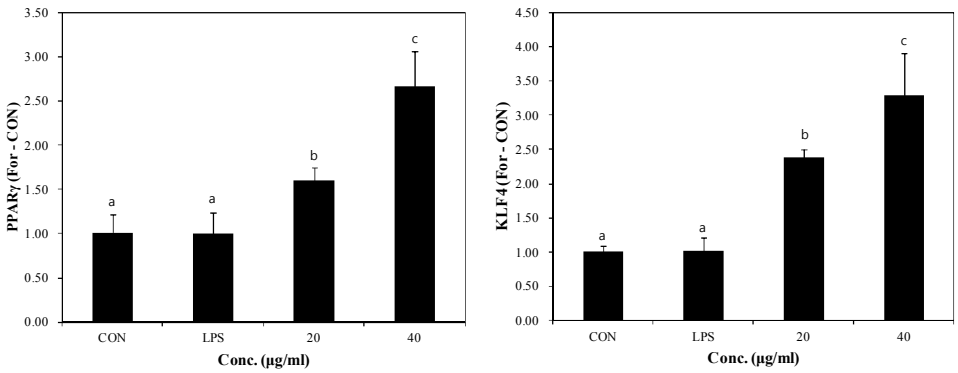

Figure 11. Effect of PYGP on the mRNA expression of the PPARγ and KLF4 following LPS-induced M1 activation. RAW 264.7 cells were pre-treated with PYGP (20 and 40 μg/mL) for 24 h and then administered 1 μg/mL LPS with PYGP (20 and 40 μg/mL) for 24 h. Values are presented as the mean ± standard deviation. Values with different letters are significantly different ($P<0.05$).

1.8 Analysis of M2 polarization markers after STAT3, STAT6 small interference RNA transfection

The STAT3 and STAT6 are major transcriptions factor that involve in the regulation of immune responses in the macrophage. It is essential for macrophage differentiation to the M2 activation. To clarify whether PYGP-mediated M2 activation in RAW 264.7 cells, we examined the expression of M2 marker after STAT3 and STAT6 gene were knock down. We tested three type of STAT3 and STAT6 siRNA, expression of STAT3 and STAT6 when using STAT3 and STAT6 siRNA-3 decreased most (STAT3; 5′-CCC GCC AAC AAA UUA AGA ATT-3′; 3′-UUC UUA AUU UGU UGG CGG GTT-5′, STAT6; 5′-CCA AGA CAA CAA CGC CAA ATT–3′; 3′-UUU GGC GUU GUU GUC UUG GTT-5′) (Fig. 12). Transfection of the RAW 264.7 with STAT3 and STAT6 siRNA decreased the PYGP induced FIZZ1, Ym1, and ARG1 mRNA expression (Fig. 13, 14). These results indicate that STAT3 and STAT6 activations are important in the RAW 264.7 macrophage switching LPS-induced M1 to M2 by PYGP.

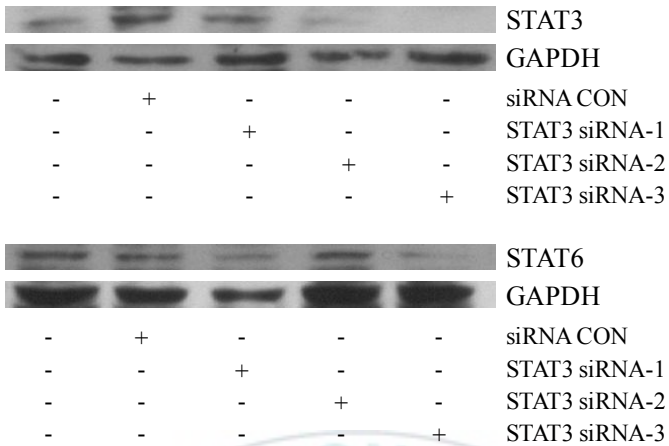

Figure 12. Effect of STAT3 and STAT6 siRNA on the expression of the STAT3 and STAT6 in RAW 264.7 cells. RAW 264.7 cells were treated with Lipofectamine and STAT3 and STAT6 siRNA for 12 h.

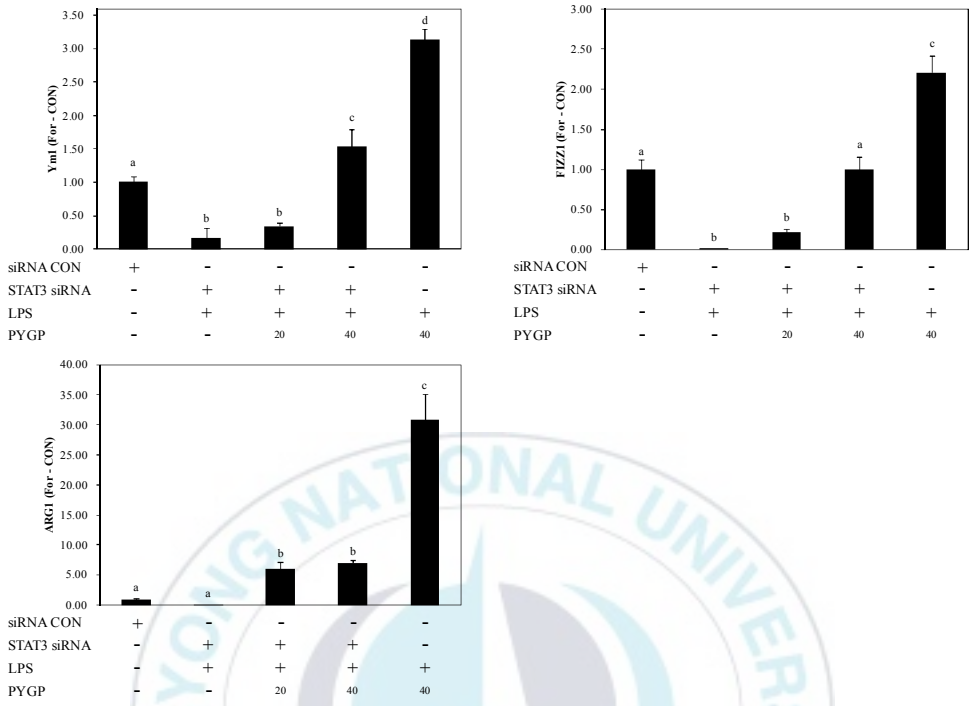

Figure 13. Effect of PYGP on the level of the M2 marker following LPS-induced M1 activation in transfected RAW 264.7. The cells were transfected with Lipofectamine and STAT3 siRNA. After transfection, cells pre-treated with PYGP (20 and 40 μg/mL) for 24 h and then administered 1 μg/mL LPS with PYGP (20 and 40 μg/mL) for 24 h. Values are presented as the mean ± standard deviation. Values with different letters are significantly different ($P<0.05$).

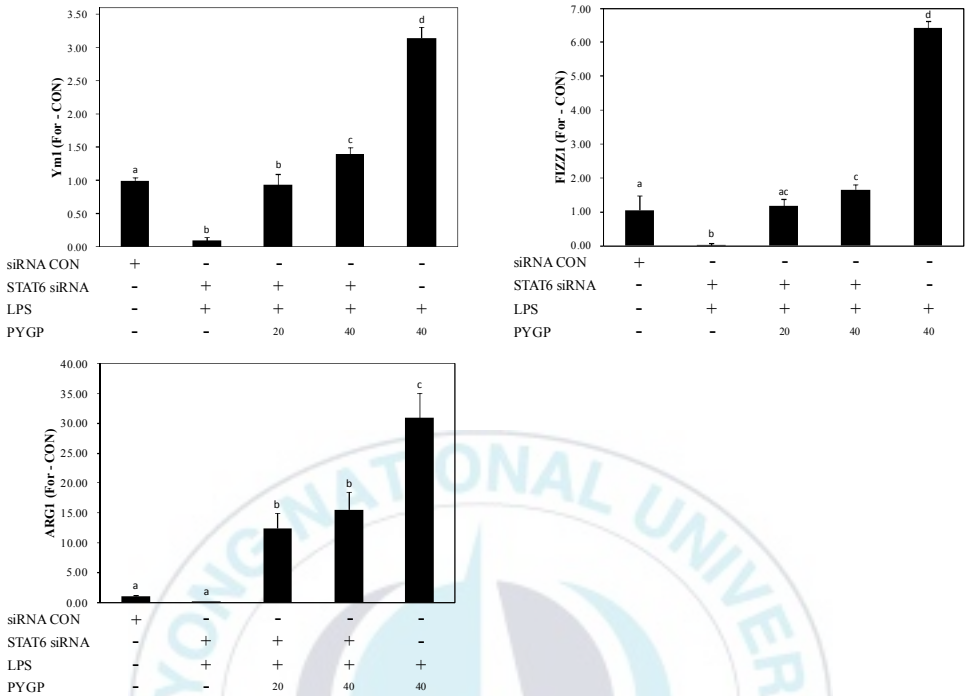

Figure 14. Effect of PYGP on the level of the M2 marker following LPS-induced M1 activation in transfected RAW 264.7. The cells were transfected with Lipofectamine and STAT6 siRNA. After transfection, cells pre-treated with PYGP (20 and 40 μg/mL) for 24 h and then administered 1 μg/mL LPS with PYGP (20 and 40 μg/mL) for 24 h. Values are presented as the mean ± standard deviation. Values with different letters are significantly different ($P<0.05$).

1.9 Discussion

Macrophage is central role in the early stages of the adaptive immune, innate immune, and regulation of inflammation. Macrophage state can divide M0 (not stimulated state), M1 (classical activation), and M2 (alterative activation) (Labonte *et al*., 2014). M1 macrophage promotes production of pro-inflammatory cytokine such as IL-1β, IL-6, TNF-α, IL-12, IFN-γ by IFN, TNF, GM-CSF, TLRs ligands stimulations (Krausgruber *et al*., 2011; Lawrence and Natoli, 2011). M2 has wound healing and anti-inflammation function and secrete IL-1ra, IL-10, TGF-β by IL-4, IL-13, IL-10, glucocorticoids, M-CSF stimulations (Biswas and Mantovani, 2010).

LPS is major M1 activation substance via TLR4 stimulation in macrophage (Verreck *et al*., 2004). LPS-activated M1 macrophage produces NO, PGE_2 and protect host against infections. But, abnormal and chronic production of NO, PGE_2 causes the various diseases (Agard *et al*., 2013; Kilbourn and Griffith, 1992). In this study, we measured that LPS significantly increased NO, PGE_2 production, which were attenuated by pre-treated PYGP in RAW 264.7 cells.

Classical activation of M1 macrophage increases aerobic glycolysis, glucose uptake and conversion of pyruvate to lactate (Hard G, 1970). Moreover, this pathway is upregulate ROS production from mitochondria via NADPH oxidase activation (West *et al*., 2011). Lipid peroxidation produced ROS caused cellular injury by inactivation of membrane enzymes and receptor (Jacobson M, 1996). In the present study, levels of their production, ROS, TBARS were increased in the LPS treatment group compared with control group. However, pre-treated PYGP group was significantly decreased

the LPS-induced ROS, TBARS level upregulation.

M1 and M2 macrophage are not only function, there is a large difference in the metabolism. The main differentiation between M1 and M2 is L-arginine metabolism. L-arginine had three pathway metabolism including NO production by iNOS, ureum and L-ornithine by arginase and agmatine by arginine decarboxylase (Corraliza *et al*., 1995; Munder *et al*., 1998; Galván-Peña and O'Neill, 2014). These characteristics can be utilized in macrophages active state. Lipid metabolism also difference in M1 and M2. This differentiation is revealed by transcriptional profiling of IL-13-steered human monocyte (Scotton *et al*., 2005). The function of these genes not fully understood such as FIZZ. PPAR ligation was reported can inhibit the expression of pro-inflammatory cytokine and iNOS (Raes *et al*., 2002; Ricote *et al*., 2000). Futhermore, they observed the difference of cytokine secretion. M1 secrete pro-inflammatory cytokines such as IL-12, IL-6, IL-1β and type 1 IFN, while M2 are secrete anti-inflammatory cytokines IL-10 and TGF-β (Mantovani *et al*., 2004). In addition, IL-4, IL-13, and IL-10 upregulate several non-opsonic receptors such as mannose receptor (CD206), CD163 (Brown *et al*., 2012; Lau *et al*., 2004). These features have been used in many studies as markers to distinguish between the activity of the macrophages (Chen *et al*., 2014; Lee *et al*., 2014; Lopez-Castejón *et al*., 2011). In the present study, LPS upregulated pro-inflammatory cytokine including IL-12, IL-6, IFN-γ, TNF-α, IL-16, IL-1β, and GM-CSF. However, pre-treatment of PYGP downreglated these pro-inflammatory cytokine and increased M2-association marker such as CD206, CD163, Ym1, FIZZ1, and ARG1. These results suggest that PYGP help to switch LPS-induced M1

classical activation to M2 alternative activation.

M2 activation has involved various transcription factors. The STAT3 and STAT6 play a key role in M2 activation (Lawrence and Natoli, 2011; Wang, N. *et al*., 2014). STAT3 is the major anti-inflammatory mediator, mediate IL-10 transcription (Murray J., 2006). Knockdown of STAT3 and STAT6 in mouse and human macrophage was reported be switched to M2 phenotype decreased significantly (Mandal *et al*., 2011; MacKinnon *et al*., 2008; Gordon and Martinez, 2010). In the present study, silencing of STAT3 and STAT6 inhibited the effect of PYGP induced mRNA expression of M2 activation marker including FIZZ1, Ym1, and ARG1. According to our observation, that STAT3 and STAT6 siRNA decrease STAT3, STAT6 protein, FIZZ1, Ym1, and ARG1 mRNA expression in the PYGP-treated M1 macrophage indicate that PYGP treatment on M1 activated macrophage was switched in to M2 macrophage via STAT3 and STAT6 signaling.

In conclusion, our results have demonstrated that in LPS-induced M1 activated macrophage. PYGP modulates inhibit pro-inflammatory cytokine and switch to M2 phenotype via STAT3 and STAT6 activation. These findings may provide a molecular basis for the ability of PYGP serving as a promising candidate for treating LPS-induced inflammatory diseases.

2. Protective effect of PYGP on D-GalN-induced cytotoxicity in Hepa 1c1c7 cells

2.1 Effect of PYGP on D-GalN-induced cytotoxicity

The protective effect of PYGP against D-GalN-induced hepatotoxicity in Hepa 1c1c7 cell was measured using the MTS cell viability assay (Fig. 15). Cells were pre-treated with PYGP for 24 h and then incubated with D-GalN and PYGP for 24 h. The results of the MTS assay showed that D-GalN treatment induced Hepa 1c1c7 cell death, whereas pre-treatment with PYGP significantly attenuated the cytotoxic effects of D-GalN.

LDH is a soluble enzyme located in the cytosol, which is released into the surrounding culture medium upon cell damage. The results of the present study demonstrated that the D-GalN-only treatment group showed increased LDH levels compared with those of the control group. By contrast, the PYGP pre-treatment groups showed significantly decreased LDH enzyme release compared with that of the D-GalN only treatment group (Fig. 16).

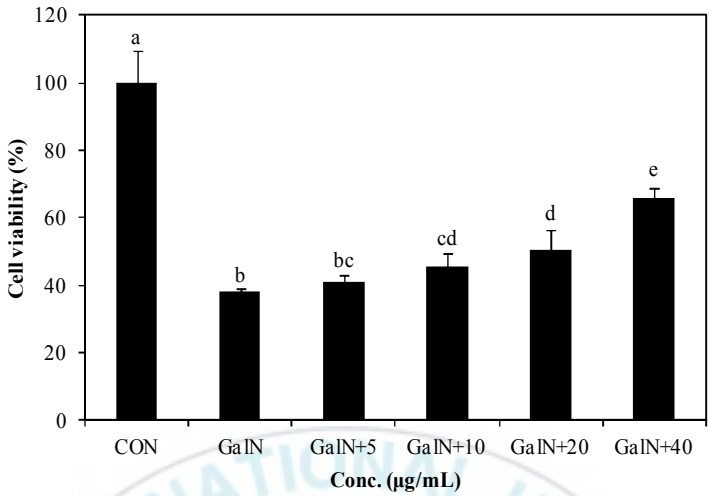

Figure 15. Effect of PYGP on D-GalN-induced cytotoxicity in Hepa 1c1c7 cells. Cells were pre-treated with PYGP (5, 10, 20, and 40 μg/mL) for 24 h and then treated with 20 mM D-GalN with PYGP (5, 10, 20, and 40 μg/mL) for 24 h. Cell viability was determined following D-GalN-induced cell cytotoxity. Values are presented as the mean ± standard deviation. Values with different letters are significantly different ($P<0.05$).

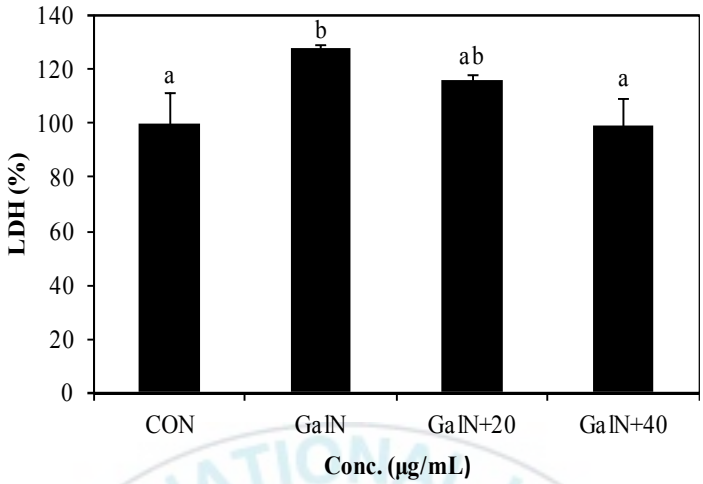

Figure 16. Effect of PYGP on D-GalN induced cytotoxicity in Hepa 1c1c7 cells. Cells were pre-treated with PYGP (20 and 40 μg/mL) for 24 h and then treated with 20 mM D-GalN with PYGP (20 and 40 μg/mL) for 24 h. Released LDH levels were determined following D-GalN induced cell cytotoxity. Values are presented as the mean ± standard deviation. Values with different letters are significantly different ($P<0.05$).

2.2 Effect of PYGP on D-GalN-induced TBARS production

Lipid peroxidation induces TBARS generation and cell damage through oxidative stress. In addition, TBARS and lipid peroxide produced during oxidative stress may cause or aggravate diseases associated with aging and hepatotoxicity. The results of the present study revealed that levels of TBARS were increased in the D-GalN-only treatment group compared with those of the control group. In addition, pre-treatment with PYGP significantly inhibited the D-GalN-induced TBARS level upregulation (Fig. 17).

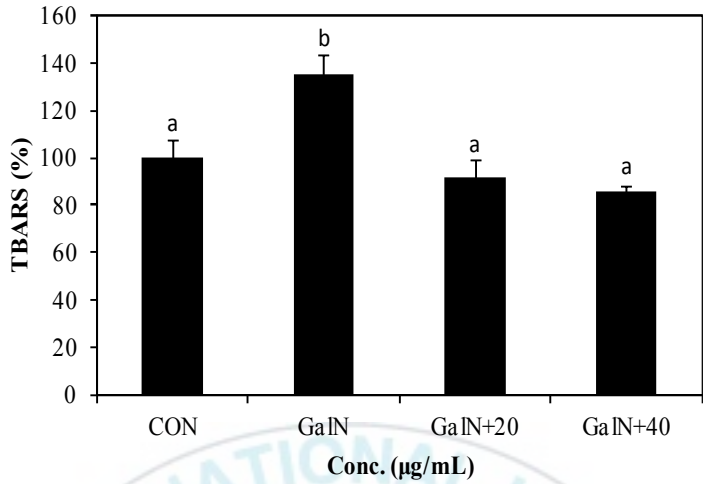

Figure 17. Effect of PYGP on D-GalN induced lipid peroxidation. Hepa 1c1c7 cells were pre-treated with PYGP (20 and 40 μg/mL) for 24 h and then administered 20 mM D-GalN with PYGP (20 and 40 μg/mL) for 24 h. Cell pellets were then collected using 1X butyl hydroxyl toluene homogenized on ice using a TBARS assay kit. Values are presented as the mean ± standard deviation. Values with different letters are significantly different ($P<0.05$).

2.3 Effect of PYGP on D-GalN-induced antioxidant enzyme activity decline

SOD, CAT, and GST are the primary defensive enzymatic anti-oxidants in eukaryotic cells. The activity levels of these enzymes were all found to be significantly inhibited in the D-GalN-only treatment group compared with those in the control group. By contrast, the PYGP pre-treatment group showed increase of SOD (Fig. 18), CAT (Fig. 19), and GST (Fig. 20) antioxidant enzyme activity compared with that in the D-GalN-only treatment group.

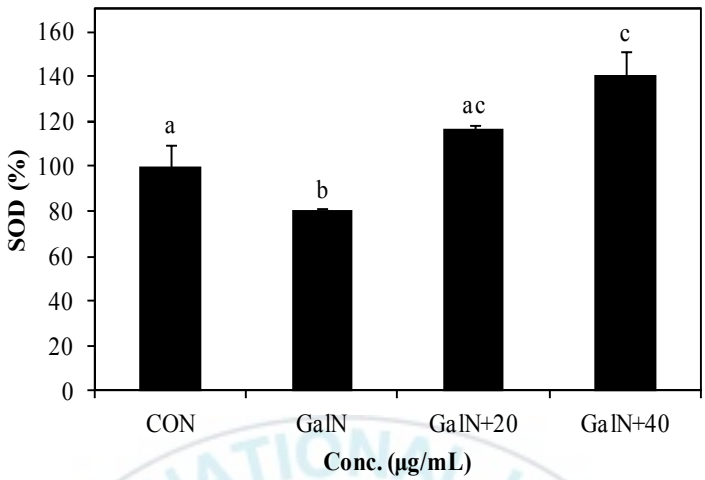

Figure 18. Effect of PYGP on the activity of the antioxidant enzymes SOD following D-GalN induced cytotoxicity. Hepa 1c1c7 cells were pre-treated with PYGP (20 and 40 μg/mL) for 24 h and then administered 20 mM D-GalN with PYGP (20 and 40 μg/mL) for 24 h. Values are presented as the mean ± standard deviation. Values with different letters are significantly different ($P<0.05$).

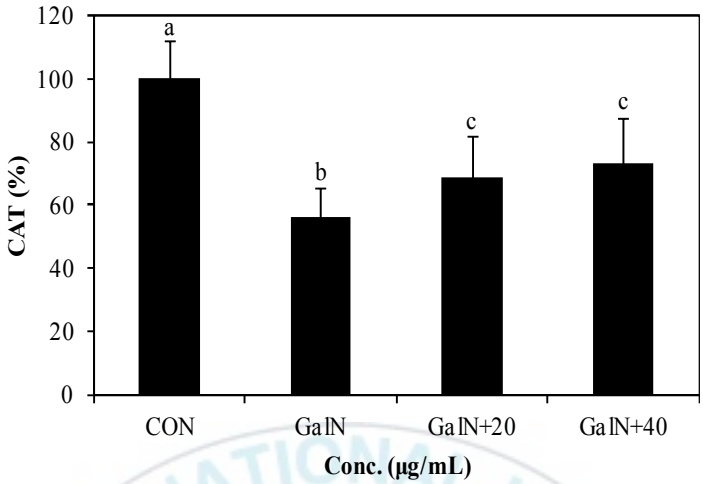

Figure 19. Effect of PYGP on the activity of the antioxidant enzymes CAT following D-GalN induced cytotoxicity. Hepa 1c1c7 cells were pre-treated with PYGP (20 and 40 μg/mL) for 24 h and then administered 20 mM D-GalN with PYGP (20 and 40 μg/mL) for 24 h. Values are presented as the mean ± standard deviation. Values with different letters are significantly different ($P<0.05$).

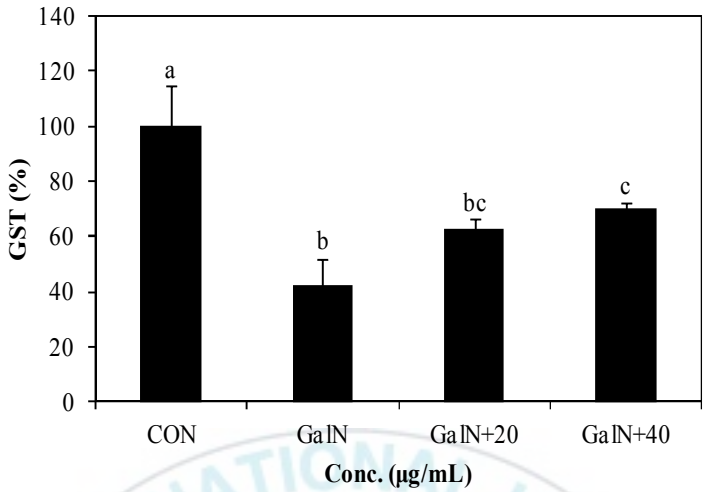

Figure 20. Effect of PYGP on the activity of the antioxidant enzymes GST following D-GalN induced cytotoxicity. Hepa 1c1c7 cells were pre-treated with PYGP (20 and 40 μg/mL) for 24 h and then administered 20 mM D-GalN with PYGP (20 and 40 μg/mL) for 24 h. Values are presented as the mean ± standard deviation. Values with different letters are significantly different ($P<0.05$).

2.4 Effect of PYGP on D-GalN-induced MAPK signaling pathway

ERK, JNK, and p38 MAPK are known to be phosphorylated and activated in response to D-GalN. In the present study, the phosphorylation of each MAPK was examined using western blot analysis. The results revealed that PYGP suppressed the D-GalN-induced phosphorylation of each MAPK. In addition, treatment with 40 μg/mL PYGP was observed to have a more suppressive effect compared with that of 20 μg/mL PYGP. However, total ERK, JNK, and p38 protein expression levels were not altered following treatment with D-GalN or PYGP pre-treatment (Fig. 21).

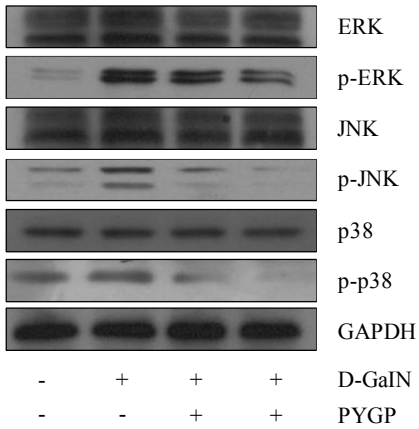

Figure 21. Effect of PYGP on D-GalN induced expression and phosphorylation of MAPK in Hepa 1c1c7 cells. Cells were pre-treated with PYGP (20 and 40 μg/mL) for 24 h and then administered 20 mM D-GalN with PYGP (20 and 40 μg/mL) for 24 h. Cell pellets were then collected using lysis buffer and western blot analysis was performed in order to determine the total protein expression and phosphorylation levels of ERK, JNK, and p38.

2.5 Effect of PYGP on Nrf2 signaling pathway

Nrf2 has previously been reported to increase the expression of various oxidant defense proteins, including HO-1, Nqo1, and GST. In the present study, western blot analysis was used to examine the expression of these proteins following D-GalN-induced cell injury and pre-treatment with PYGP. Cells exposed to D-GalN-only reduced Nrf2, HO-1, Nqo1, and GST protein expression levels compared with those of the untreated cells. By contrast, the expression of these Nrf2-stimulated proteins following PYGP pre-treatment were significantly increased compared with those in the D-GalN-only group (Fig. 22).

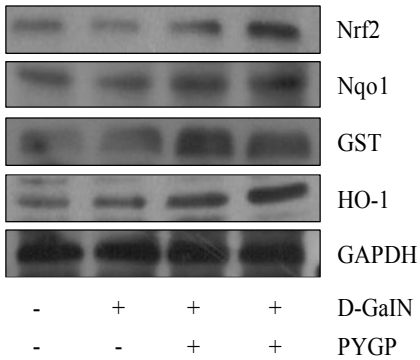

Figure 22. Effect of PYGP on D-GalN induced expression of Nrf2, Nqo1, GST, and HO-1 in Hepa 1c1c7 cells. Cells were pre-treated with PYGP (20 and 40 μg/mL) for 24 h and then administered 20 mM D-GalN with PYGP (20 and 40 μg/mL) for 24 h. Cell pellets were then collected using lysis buffer and western blot analysis was performed in order to determine protein expression levels of Nrf2, Nqol, GST, and HO-1.

2.6 Discussion

In the present study, cytotoxic injury was induced in Hepa 1c1c7 cells using D-GalN, which is a commonly used model for screening anti-hepatotoxic and anti-hepatoxic activities of drugs. D-GalN-induced liver injury has previously been shown to closely resemble acute viral hepatitis (Decker and Keppler, 1971; Nakagiri *et al*., 2003). D-GalN has direct and indirect roles, which affect the oxidative stress properties of organs. Several studies have shown that D-GalN induced changes in liver antioxidant enzyme levels (Pushpavalli *et al*., 2010; Han *et al*., 2006; Shi *et al*., 2008; Lim *et al*., 2000). In addition, D-GalN was reported to induce hepatotoxicity by inhibiting RNA and protein synthesis as well as reducing uridine 5'-triphosphate, uridine 5'-diphosphate, and uridine 5'-monophosphate levels (Tang *et al*., 2004; Aristatile *et al*., 2011). Increased LDH release into the medium as a result of cell damage is widely used as a measure of cytotoxicity (Liu and Yeh, 2000). In the present study, D-GalN treatment was found to induce cytotoxicity in Hepa 1c1c7 cells, the effect of which was attenuated in cells pre-treated with PYGP.

Peroxidation of endogenous lipids is a major factor affecting the cytotoxic activity of D-GalN (Das *et al*., 2012). D-GalN induced oxidative stress damage is generally attributed to the formation of highly reactive hydroxyl radicals, such as superoxide anions, which stimulate lipid peroxidation and damage to cell membranes (Halliwell and Gutteridge, 1984). In the present study, TBARS was significantly increased following D-GalN-only treatment; however, pre-treatment with PYGP decreased the oxidative damage in cells, based on the decreased levels of TBARS

compared to those in the D-GalN-only group. SOD and CAT are fist-line cellular antioxidant defense enzymes. SOD reacts with O_2 in order to generate H_2O_2 and H_2O (Mallick and Mohn, 2000), while CAT accelerates the dismutation reaction of H_2O_2 and the formation of H_2O and O_2 (Jones and Suggett, 1968; Halliwell B, 1999). GST binds to numerous different lipophilic drugs and chemicals. Thus, it likely binds to D-GalN and functions as an enzyme for GSH conjugation reactions (Anandan *et al*., 1998). In the present study, D-GalN-induced lipid peroxidation was measured; following 24 h of exposure to D-GalN, there was a significant increase in TBARS levels compared with those of the control group. However, the PYGP pre-treatment groups showed reduced TBARS levels compared with those in the D-GalN-only group. Furthermore, D-GalN significantly decreased the activity levels of the antioxidant enzymes CAT, GST, and SOD compared with those in the control group, while pre-treatment with PYGP increased these enzyme levels compared with those in the D-GalN-only treatment group.

The MAPK signaling pathway is an important signaling pathway which regulates tumor necrosis factor (TNF)-α expression; however, the detailed mechanism of this remains to be fully elucidated (Guha and Mackman, 2001; Kawai and Akira, 2007). MAPK have been confirmed to participate in regulating cytokine production in response to a broad range of stimuli (Guan K, 1994; Johnson *et al*, 2005). MAPK include three major proteins: ERK, JNK, and p38 MAPK. These proteins have important biological roles in cell proliferation, differentiation, metabolism, survival, and apoptosis (Kim and Choi, 2010). In the present study, levels of their activated forms, p-ERK, p-JNK, and p-p38, were observed to be increased in the

D-GalN-only treatment group compared with those in the untreated control group; however, PYGP pre-treatment attenuated the D-GalN mediated activation of ERK, JNK, and p38.

As a transcription factor, Nrf2 promotes the translation of genes which have a protective effect against oxidative/electrophilic stress (Klaassen and Reisman, 2010; Inoue *et al*, 2012). Nrf2 exists as a binding repressor of kelch-like erythroid cell-derived protein with CNC homology-associated protein 1 (Keap 1) in the cytoplasm (Jaiswal A, 2004). In response to oxidative stress, Nrf2 dissociates from Keap 1, and translocates to the nucleus in order to induce an array of cytoprotective genes, including Nqo1, GST, and HO-1 (Kensler *et al*., 2007; Wu *et al*., 2012). In the present study, western blot analysis revealed that Nrf2, Nqo1, GST, and HO-1 expression levels were decreased in the presence of D-GalN. However, PYGP pre-treatment increased Nrf2, Nqo1, GST, and HO-1 expression levels compared with those in the D-GalN-only treatment group. These results indicated that PYGP pre-treatment upregulated Nrf2 protein levels and stimulated the activity of antioxidants and phase II detoxifying enzymes.

In conclusion, the results of the present study demonstrated that PYGP reduced D-GalN induced hepatotoxicity in Hepa 1c1c7 hepatocytes via upregulation of antioxidative enzymes, MAPK, and the Nrf2 pathway. These fidings therefore indicated that PYGP may have potential for use for the prevention of hepatotoxicity.

3. Protective effect of PYGP on D-GalN-induced toxicity in primary rat hepatocyte

3.1 Effect of PYGP on primary liver cell viability

The effect of PYGP treatment on LDH in liver primary culture cells were using LDH kit (Fig. 23). Destroyed cell or severe damaged cell is release LDH to extracellular. Therefore, LDH level was one of most using to determine hepatocyte injury. The concentration level of LDH increased in D-GalN-only group compared with CON group. PYGP treatment significantly dose-dependent decreased LDH level.

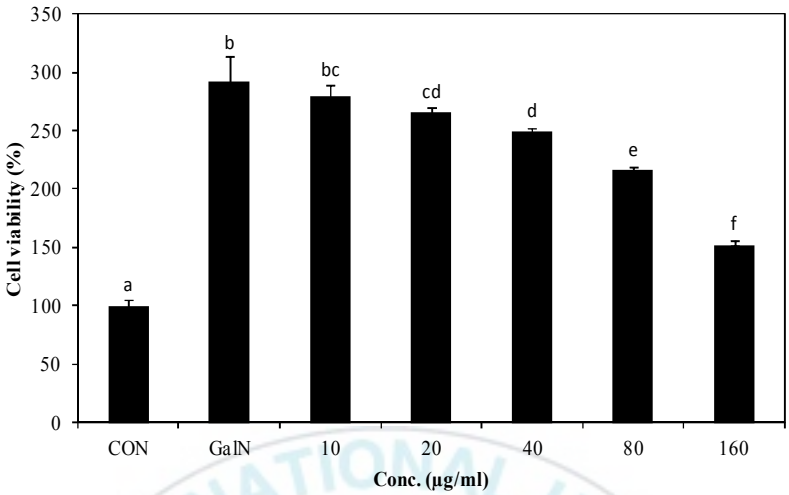

Figure 23. Effect of PYGP on D-GalN induced cytotoxicity in primary culture hepatocyte. Cells were pre-treated with various concentration of PYGP (10, 20, 40, 80, and 160 μg/mL) for 24 h and then treated with 25 mM D-GalN with PYGP (10, 20, 40, 80, and 160 μg/mL) for 24 h. Released LDH levels were determined following D-GalN induced cell cytotoxity. Values are presented as the mean ± standard deviation. Values with different letters are significantly different ($P<0.05$).

3.2 Effect of PYGP on D-GalN-induced MAPK signaling pathway

MAPK signal pathway is important in D-GalN hepatotoxicity. D-GalN treatment lead to phosphorylation of ERK, JNK, and p38 proteins. Phosphorylated ERK, JNK, and p38 were significantly increased by D-GalN expose, while the total protein expression was almost same in each groups (Fig. 24). These results revealed that PYGP attenuate the D-GalN-induced phosphorylation of MAPK protein.

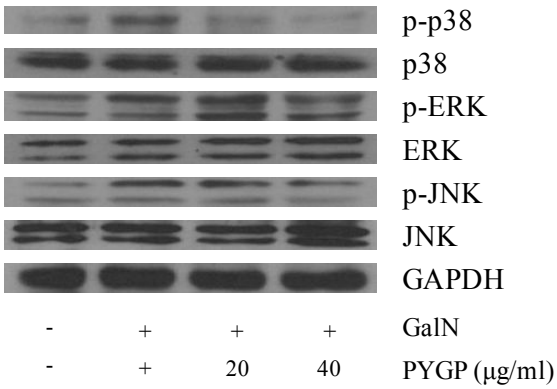

Figure 24. Effect of PYGP on the expression of the MAPK pathway following D-GalN induced hepatotoxicity. Primary hepatocyte was pre-treated with PYGP (80 and 160 μg/mL) for 24 h and then administered 25 mM D-GalN with PYGP (80 and 160 μg/mL) for 24 h. Values are presented as the mean ± standard deviation. Values with different letters are significantly different ($P<0.05$).

3.3 Discussion

D-GalN is frequently used as *in vitro* and *in vivo* experimental hepatotoxicity model. The treatment of D-GalN to the cells or animal induces the liver cells damage and leads to inhibition of RNA, protein synthesis by uridine pool depletion. This injury was reported closely resembling viral hepatitis (Nakagiri *et al*., 2003). Different hepatotoxic model such as cell line, mouse and another animal model were frequently used as prove the effectiveness of a drug. However, considering the economic or ethical reason, efficiently experimental models are required. Isolated rat hepatocytes or primary culture model can provide similar environment of actual in vivo, it suitable for observing the mechanisms of the drugs (Kučera *et al*., 2006).

D-GalN-induced hepatotoxicity elevate to LDH level in culture medium (Fouad *et al*., 2004). While the incubation of primary hepatocyte with D-GalN was upregulated the level of LDH. D-GalN with PYGP co-treatment group LDH level was significantly decreased in the dose-dependent manner. These results indicated that PYGP treatment cause the proccess of attenuating D-GalN-induced cytotoxicity in primary hepatocyte.

The MAPK signaling pathway was reported as an important mediators of cell proliferation, apoptosis, and cell survive. Moreover, MAPK was correlated with diverse chemical stimulus such as carbon tetrachloride, acetaminophen, and ethanol. The activation of JNK is associated with cell death and liver oxidative injury, ERK is reported an important role in oxidative stress injury and cell inflammation. Although, the activation of p38 is linked with inflammation, apoptosis, and cell differentiation (Kim and

Choi, 2010). In the present study, phosphorylation of JNK, ERK, and p38 upregulate by D-GalN treatment. These MAPK protein phosphorylation was significantly decreased PYGP pretreatment.

These results indicated that PYGP pretreatment attenuated the D-GalN-induced liver injury via MAPK signal pathway. Moreover, these results shown a similar disposition as our previous study (Hepa 1c1c7 cells). We obtained similar results using another sequence protein samples in this model. Therefore, it is considered to be useful in models which can be studied physiological properties of the drug in the liver.

4. PYGP regulates antioxidant status and prevents hepatotoxicity in D-GalN/LPS-induced acute liver failure in rats

4.1 Effect of PYGP on GOT and GPT level in serum

GOT and GPT levels in the serum are important indicators of liver function. D-GalN/LPS injection elevated the levels of both, and administration of 300 mg/kg/BW PYGP significantly reduced their respective increases (Fig. 25).

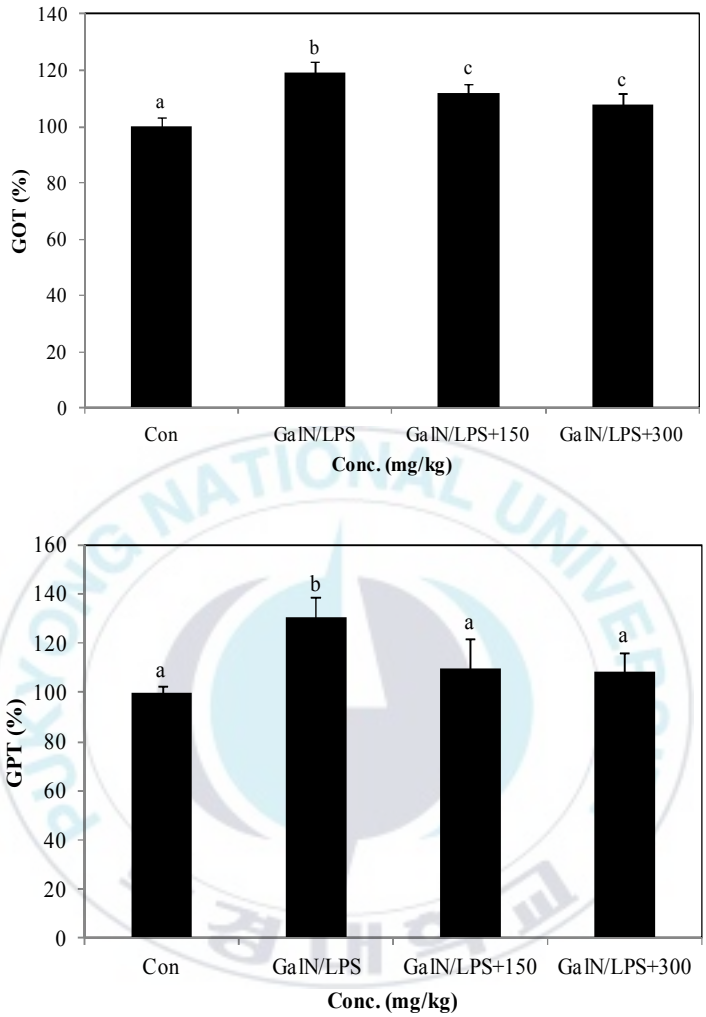

Figure 25. GOT and GPT levels in the serum of control and experimental rat groups. Values are presented as the mean ± standard deviation. Values with different letters are significantly different ($P<0.05$).

4.2 Effect of PYGP on D-GalN/LPS-induced oxidative stress and antioxidant enzymes

Six hours after D-GalN/LPS injection, we determined the TBARS level, which indicates liver tissue lipid peroxidation. As shown in Figure 26, TBARS increased significantly after D-GalN/LPS treatment. The D-GalN/LPS+PYGP 150 and D-GalN/LPS+PYGP 300 groups showed that marked upregulation of TBARS level. Furthermore, CAT (Fig. 27), GST (Fig. 28), and GSH (Fig. 29) were also decreased by D-GalN/LPS treatment, but recovered to levels similar to the control group by PYGP treatment.

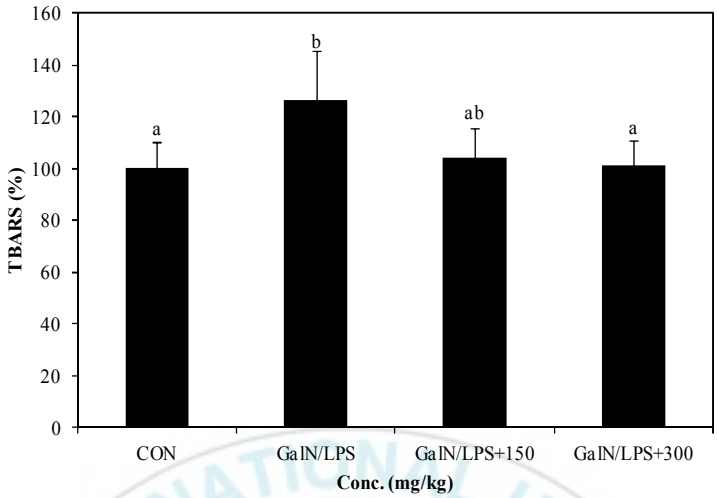

Figure 26. Effect of PYGP on the level of the TBARS following D-GalN/LPS induced liver injury. Rats were treated as materials and methods. Values are presented as the mean ± standard deviation. Values with different letters are significantly different ($P<0.05$).

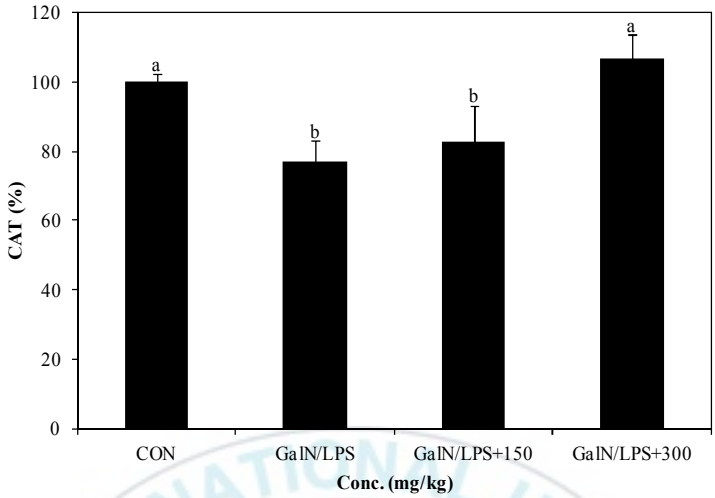

Figure 27. Effect of PYGP on the activity of the CAT following D-GalN/LPS induced liver injury. Rats were treated as materials and methods. Values are presented as the mean ± standard deviation. Values with different letters are significantly different ($P<0.05$).

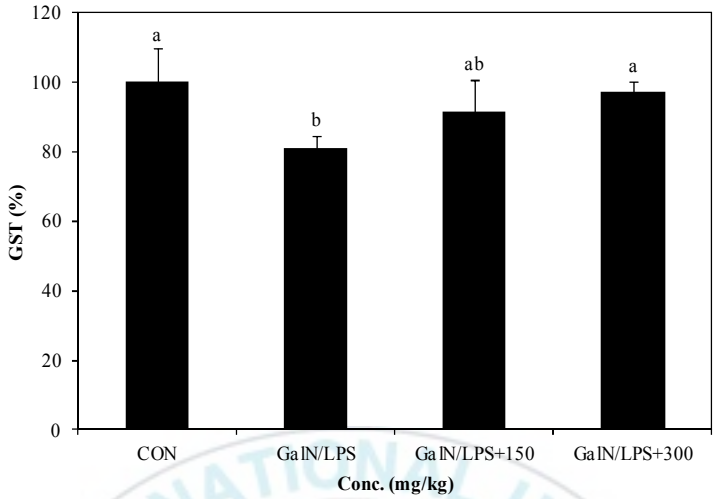

Figure 28. Effect of PYGP on the activity of the GST following D-GalN/LPS induced liver injury. Rats were treated as materials and methods. Values are presented as the mean ± standard deviation. Values with different letters are significantly different ($P<0.05$).

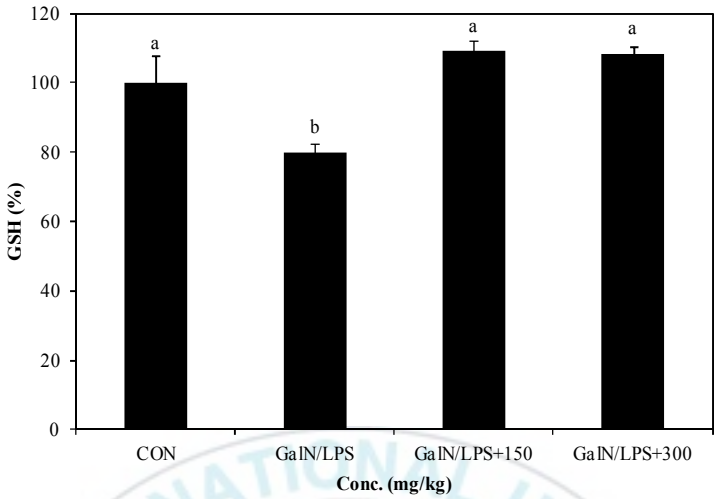

Figure 29. Effect of PYGP on the level of the GSH following D-GalN/LPS induced liver injury. Rats were treated as materials and methods. Values are presented as the mean ± standard deviation. Values with different letters are significantly different ($P<0.05$).

4.3 Effect of PYGP on D-GalN/LPS-induced MAPK phosphorylation

To investigate whether PYGP can modulate the MAPK signaling pathways, we determined MAPK protein expression and phosphorylation using Western blot assays. The expressions of ERK, JNK, and p38 proteins were not different between groups. However, their phosphorylation increased in the D-GalN/LPS-treated group compare with the control group. In the D-GalN/LPS+PYGP co-treated groups, their levels were downregulated (Fig. 30). These results suggest that PYGP inhibits D-GalN/LPS-induced MAPK phosphorylation.

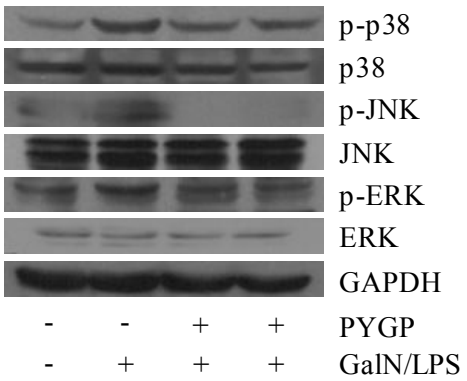

Figure 30. Expression of MAPK protein in the livers of control and experimental rat groups. Livers were collected in lysis buffer and Western blot analysis was performed to determine the total protein expression and phosphorylation levels of ERK, JNK, and p38 MAPK.

4.4 Effect of PYGP on iNOS and COX-2 protein expression

To confirm the effects of PYGP on inflammatory responses in the rat liver, we examined D-GalN/LPS-induced iNOS and COX-2 protein expression. When rats were treated with D-GalN/LPS, protein expression levels significantly increased. Treatment with PYGP prior to injection of D-GalN/LPS inhibited D-GalN/LPS-induced iNOS and COX-2 protein expression (Fig. 31). These results suggest that PYGP plays an important role in the suppression of D-GalN/LPS-induced iNOS and COX-2 protein expression.

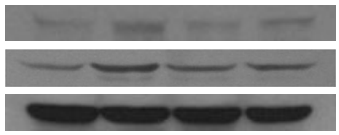

Figure 31. Expression of iNOS and COX-2 protein in the livers of normal and experimental rat groups. Livers were collected in lysis buffer and Western blot analysis was performed to determine the total protein expression of iNOS and COX-2.

4.5 Discussion

Treating rats with a combination of D-GalN/LPS is widely used to study the mechanisms of human ALF (Gilani *et al*., 2005). D-GalN and LPS co-treatment induces greater critical damage accompanied with apoptotic and necrotic changes in the liver, which closely resemble human viral hepatitis (Liu *et al*., 2008; Vimal and Devaki, 2004). In the present study, administration of D-GalN/LPS cause GOT and GPT levels increase in the serum. However, orally injected PYGP attenuated their levels. These results suggest that D-GalN/LPS induces severe damage to hepatic membrane tissues, and PYGP prevents this hepatic toxicity.

D-GalN/LPS hepatotoxicity induces the production of ROS and a loss of antioxidative enzymes in the liver (Wang *et al*., 2007). Moreover, ROS may cause cell membrane lipid peroxidation (Bindhumol *et al*., 2003). Oxidative stress is a well-known factor in D-GalN/LPS-induced liver injury. Increased TBARS and conjugated dienes have previously been detected following treatment with D-GalN/LPS (Lekić *et al*., 2011). In the present study, TBARS level increased in response to D-GalN/LPS treatment. However, co-treatment with D-GalN/LPS and PYGP suppressed hepatic TBARS levels. Antioxidant enzymes, including CAT, GST, and GSH are important in D-GalN/LPS hepatotoxicity. CAT catalyzes the dismutation reaction of H_2O_2 and the formation of H_2O and O_2 (Vimal and Devaki, 2004). GST catalyzes the conjugation of glutathione (GSH) with drugs and chemicals (Nordberg and Arnér, 2001). In the present study, treatment with D-GalN/LPS significantly reduced the activities of CAT and GST, as compared with control group. Conversely, increased CAT and GST activities, and GSH

levels were detected following PYGP treatment. These results suggested that PYGP exerts antioxidative effects against D-GalN/LPS-induced liver injury.

MAPK comprise ERK, JNK, and p38 proteins, which are phosphorylated by D-GalN/LPS (Chen *et al*., 2012). These proteins are involved in cell proliferation, differentiation, metabolism, survival, and apoptosis (Pearson *et al*., 2001). In particular, these proteins regulate cytokine production and transcription factors (Aggarwal B, 2004; Tak and Firestein, 2001). In the present study, treatment with PYGP significantly suppressed the D-GalN/LPS-induced phosphorylation of ERK, JNK, and p38 proteins. These results indicated that D-GalN/LPS and PYGP co-treatment reduce MAPK phosphorylation.

Inflammation reactions occur through various biological pathways. NO production occurs via the iNOS pathway (Ishizaki *et al*., 2008); in the cell, increased iNOS protein expression produces large amounts of NO, which increases the prevalence of inflammation (Xia *et al*., 2014). In addition, overexpression of NO induces hepatic dysfunction and hepatotoxicity (Li *et al*., 2011). COX-2 is associated with the pathophysiology of inflammatory dysfunctions, and the production of prostaglandins and thromboxanes (Serhan and Oliw, 2001), which may lead to hepatic injury (Huang *et al*., 2013). In the present study, PYGP pretreatment inhibited D-GalN/LPS-induced iNOS and COX-2 overexpression.

In conclusion, the present study demonstrated that PYGP may exert protective effects against D-GalN/LPS-induced ALF via inhibition of MAPK phosphorylation and iNOS and COX-2 expression. In addition, PYGP increased the activity of antioxidant enzymes.

5. Protective effect of PYGP on ethanol-induced hepatotoxicity in rat

5.1 Effect of PYGP on GOT and GPT level in serum

In hepatotoxicity, serum GOT and GPT levels were increased by liver injury or liver cell destroy. The results of the present study revealed that level of GPT and GPT were significantly increased in the chronic ethanol only consumption group compared with those of the control group. Whereas ethanol with PYGP consumption group showed decreased GOT and GPT levels (Fig. 32).

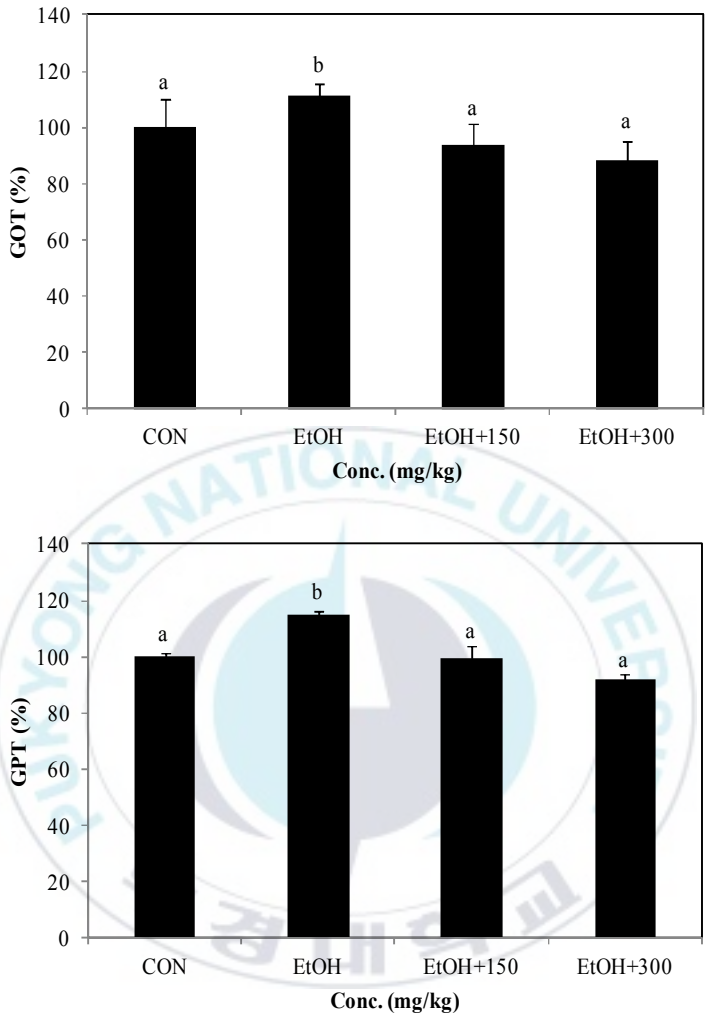

Figure 32. GOT and GPT levels in the serum of control and experimental rat groups. Values are presented as the mean ± standard deviation. Values with different letters are significantly different ($P<0.05$).

5.2 Effect of PYGP on ethanol-induced antioxidant enzyme activity decline

The activities of CAT, GSH-px, and level of GSH antioxidant enzymes were remarkably decreased in ethanol only treated group compared with the control group. In contrast, the level of GSH (Fig. 33) and activity of GSH-px (Fig. 34) were restored in ethanol with PYGP 300 mg/kg consumption group. Moreover, the activity of CAT significant increased concentration dependant manner (Fig. 35).

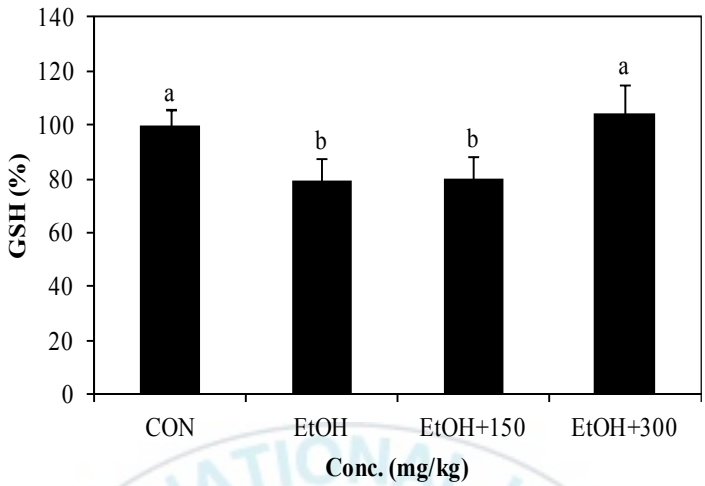

Figure 33. Levels of the antioxidant enzymes GSH in the livers of control and experimental rat groups. Values are presented as the mean ± standard deviation. Values with different letters are significantly different ($P<0.05$).

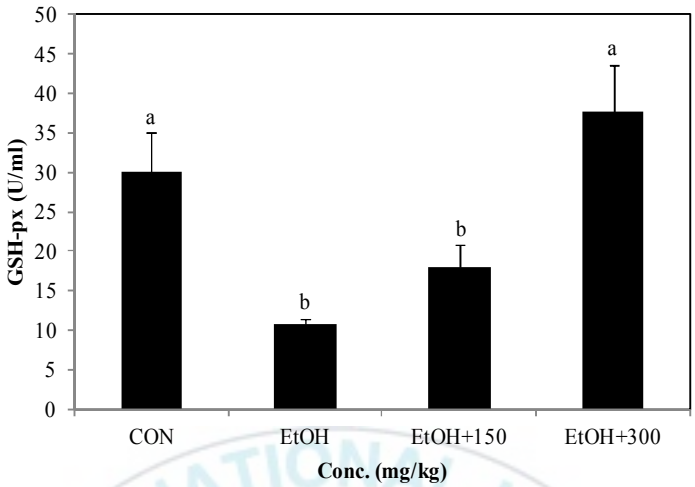

Figure 34. Levels of the antioxidant enzymes GSH-px in the livers of control and experimental rat groups. Values are presented as the mean ± standard deviation. Values with different letters are significantly different ($P<0.05$).

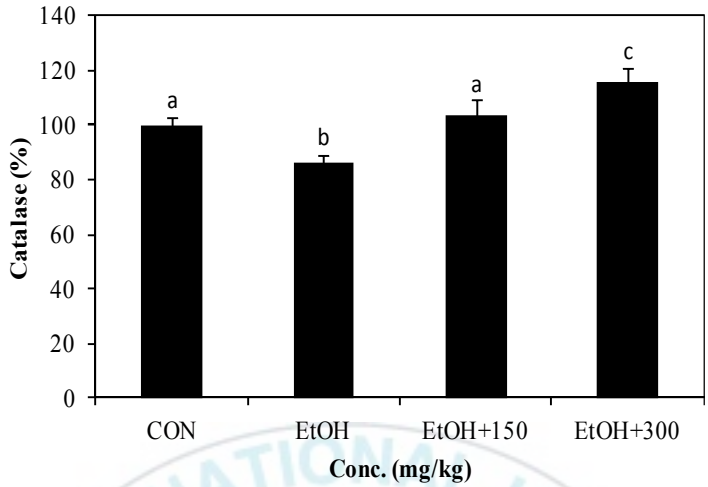

Figure 35. Levels of the antioxidant enzymes CAT in the livers of control and experimental rat groups. Values are presented as the mean ± standard deviation. Values with different letters are significantly different ($P<0.05$).

5.3 Effect of PYGP on ethanol-induced MAPK phosphorylation

To examined whether PYGP inhibit the MAPK phosphorylation, we used Western blot assays. In result, ethanol induced ERK, JNK, and p38 phosphorylation compared with the control group. PYGP was effectively inhibiting the ethanol-induced ERK, JNK, and p38 protein phosphorylation. In contrast, ethanol and PYGP were not effect on ERK, JNK, and p38 protein expressions (Fig. 36). These results suggest that PYGP can inhibit ethanol-induced MAPK phosphorylation.

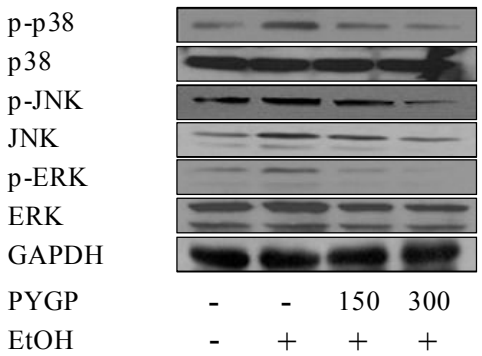

Figure 36. Expression of MAPK protein in the livers of control and experimental rat groups. Livers were collected in lysis buffer and Western blot analysis was performed to determine the total protein expression and phosphorylation levels of ERK, JNK, and p38.

5.4 Effect of PYGP on COX-2, iNOS, and CYP2E1 expression

Chronic ethanol consumption has been known that increase iNOS, COX-2, and CYP2E1 protein expressions. These proteins related liver inflammation and cell injury. In the present study, chronic ethanol consumption was up-regulated iNOS, COX-2, and CYP2E1 protein expression. By contrast, iNOS, COX-2, and CYP2E1 protein expression was decreased in chronic ethanol consumption with PYGP group (Fig. 37). This result suggest that PYGP plays an important role in the suppression of chronic ethanol-induced iNOS, COX-2, and CYP2E1 protein expression.

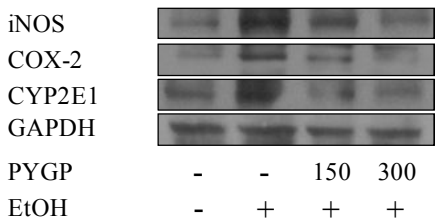

Figure 37. Expression of iNOS, COX-2, and CYP2E1 protein in the livers of normal and experimental rat groups. Livers were collected in lysis buffer and Western blot analysis was performed to determine the total protein expression of iNOS, COX-2 and CYP2E1.

5.5 Discussion

Ethanol consumption-induced pathogenesis is complicated. It is associated with oxidative stress, ROS generation, and innate immune response alteration via ethanol metabolism (Bailey and Cunningham, 2002; Hines and Wheeler, 2004; Kumar *et al*., 2011). Especially, chronic ethanol consumption in humans leads serious liver problem such as fibrosis, cirrhosis, and hepatocellular carcinoma (Leung *et al*., 2012). Increased GOT and GPT level as a result of liver injury is commonly used as a measure of hepatotoxicity. In the present study, chronic ethanol consumption was increased GOT and GPT levels in the serum, co-consumption with PYGP was attenuated like control group.

Chronic ethanol consumption induces the loss of antioxidant or diminution enzyme activity such as GSH-px, and CAT (Ostrowska *et al*., 2004). GSH composed of tripeptide and effectively scavenges ROS, free radicals (Wu *et al*., 2004). GSH-px acts catalyst in the reduction of H_2O_2 and diverse hydroperoxides with GSH in the role of electron donor (Chang *et al*., 2004). CAT plays an important role in reaction of H_2O_2 and the formation of H_2O and O_2 (Vimal and Devaki, 2004). In the present study, antioxidant enzymes GSH, GSH-px, and CAT activity levels were significantly decreased by chronic ethanol consumption, while co-consumption with PYGP increased those enzyme levels compared with ethanol-treated group.

MAPK is serine-threonine kinases that play an essential role in intracellular signal including cell proliferation, differentiation, transformation, survival, and death (Wada and Penninger, 2004). Ethanol consumption activate MAPK cascade by protein phosphorylation (Park *et al*., 2012). In

particular, these proteins regulate oxidative stress in ethanol-induced hepatotoxicity (Aroor and Shukla, 2004). In this study, we showed that ethanol consumption caused the phosphorylation of ERK, JNK, and p38 in rat liver. PYGP co-consumption group observed that attenuation of phosphorylation.

Chronic ethanol consumption increases expression of COX-2, iNOS protein in liver (Tahir *et al*., 2013). These proteins linked with ethanol-induced liver inflammatory response (Murakami and Ohigashi, 2007). Nitric oxide (NO) is a highly reactive oxidizing agents, the synthesis of NO is associated with iNOS expression (Gardner *et al*., 1998). Mainly, involved in the protective effect of such bacteria, parasites, and tumor cells, but overexpression of NO causes damage to the organ (Quan *et al*., 2011). COX-2 linked a lot of biological response such as inflammation, carcinogenesis, and hepatic fibrogenesis (Hu K, 2003). In alcoholic liver disease, COX-2 is increased in Kupffer cells (Nanji *et al*., 1997). Increased expression of COX-2 promotes the lipid peroxidation, endotoxin, synthesis of TNF-α, and Thromboxane B2 (TXB_2). In particular, TXB_2 is associated with serious alcoholic liver disease (Nanji *et al*., 1993). In the present study, iNOS, COX-2 protein expression was increased by chronic ethanol consumption, while co-consumption with PYGP was attenuate compared ethanol only group.

Chronic ethanol consumption promotes CYP2E1 production, and that generates a large amount of ROS such as H_2O_2 and O_2 (Zima and Kalousova, 2005; Lu and Cederbaum, 2008). CYP2E1 catalyze oxidizing small amount of ethanol to ADH about 10% (Ceni *et al*., 2014). ADH is believed the major toxin in ethanol-induced liver injury, inflammation, and

extracellular matrix (Seth *et al*., 2011). In the present study, chronic ethanol consumption rat showed higher level of CYP2E1 enzyme production in liver compared control group. Ethanol with PYGP administration group showed inhibition of CYP2E1 level.

In conclusion, chronic ethanol consumption was induced the hepatotoxicity and inhibition of antioxidant status in the liver such as GSH, GSH-px, and CAT. Moreover promote overexpression of iNOS, COX-2, CYP2E1, and overactivation of ERK, JNK, p38. PYGP prevented chronic ethanol consumption-induced hepatotoxicity in rat via downregulation of MAPK phosphorylation and iNOS, COX-2, CYP2E1 expression. These results represent that PYGP may use for novel treatment against chronic ethanol hepatotoxicity.

Ⅳ. DISCUSSION

Inflammation is one of major defense system in body, and physiological response against viral infections and bacterial infections (Labonte *et al*., 2014). Furthermore, Inflammation is mediated by a variety of diseases, but also plays an important role in pathological response (Sica and Mantovani, 2012). But, abnormal inflammatory response is cause of the diverse disease such as cancer, insulin resistance-related disease, and atherosclerosis (Fenyo and Gafencu, 2013; Visser *et al*., 2005; Xu *et al*., 2003).

Macrophage plays key role in the inflammatory activity and represents a different function depending on the polarization state. Macrophage state can divide M0 (not stimulated state), M1 (classical activation), and M2 (alterative activation) (Labonte *et al*., 2014). M1 macrophage promotes production of pro-inflammatory cytokine and inflammatory response. In tissue injury or infection, M1 macrophages help to removal of infected element by secrete pro-inflammatory cytokine and oxidative processes. Moreover, M1 macrophage eliminates infected and tumoral cells (Bosschaerts *et al*., 2010; Serbina *et al*., 2003). But, it can also damage to the surrounding normal cells and lead to over inflammation (Nathan and Ding, 2010). M2 macrophage promotes wound healing and anti-inflammtory response. Whereas, several studies have identified characters for M2 macrophage in allergy and asthma lead by IL-4 and IL-13 secretion (Prasse *et al*., 2007). Therefore, consideration to the characteristics of these conflicting macrophages, M1 and M2 macrophage polarization responses must be

controlled to prevent negative effect on host.

Kupffer cells (KCs) are conduct homeostatic function, tissue remodeling, damage recovering, and regulate metabolic functions (Sica and Mantovani, 2012; Mantovani *et al*., 2013). Furthermore, KCs plays a important role in the phathogenesis of alcoholic liver disease and toxic xenobiotics, and fibrosis (Sica *et al*., 2014). PYGP was observed that is inhibited the D-GalN toxicity via MAPK and Nrf2 pathway in Hepa 1c1c7 cells. In addition, PYGP was identified that the protective effect on the liver injury by ethanol and D-GalN/LPS. In animal experimental model, PYGP was observed that is being suppressed MAPK signal pathway and also inhibited inflammation responses. Moreover, PYGP inhibited the oxidative stress that occurs during the liver tissue injury. PYGP have similar effects that M2 macrophages represent the wound healing and anti-inflammatory responses in liver tissue injury. Considering these results, we established the hypothesis that the PYGP affect the macrophage polarization.

Inflammation response was induced in order to create a similar environment like animal model to macrophage using LPS. LPS is major M1 activation substance via TLR4 stimulation and inflammatory response inducer in macrophage (Verreck *et al*., 2004). LPS-activated M1 macrophage produces NO, PGE_2, ROS, TBARS and pro-inflammatory cytokine mRNA such as IL-1β, IL-6, IL-12, and type 1 IFN. In the present study, PYGP pre-treatment was downregulate NO, PGE_2, ROS, and TBARS. Moreover, IL-12, IL-6, IFN-γ, TNF-α, IL-16, IL-1β, and GM-CSF pro-inflammatory cytokine production was also decreased by PYGP pre-treatment. In addition, PYGP was increased M2 polarization marker mRNA such as CD163,

CD206, Ym1, FIZZ1, and ARG1. M2 activation has involved a various transcription factor. The STAT3 and STAT6 is the major M2 activation regulator. In the present study, silencing STAT3 and STAT6 inhibited the effect of PYGP induced mRNA expression of M2 activation marker including FIZZ1, Ym1, and ARG1. Our observation that STAT3 and STAT6 siRNA decreases STAT3, STAT6 protein, FIZZ1, Ym1, and ARG1 mRNA expression in PYGP-treated M1 macrophage indicate that the PYGP treatment on M1 activated macrophage switch to M2 macrophage via STAT3 and STAT6 signaling.

In conclusion, our results have demonstrated that PYGP was prevent to D-GalN-induced cell cytotoxicity in Hepa 1c1c7 cells and it was prevent to D-GalN/LPS and ethanol-induced hepatotoxicity in animal liver injury models. In addition, PYGP modulates inhibit pro-inflammatory cytokine and switch to M2 phenotype via STAT3 and STAT6 activation in LPS-induced M1 activated macrophage. These results suggest that protective effect of hepatotoxicity by PYGP is closely related to macrophage polarization switch. Therefore, we suggest the possibility of PYGP to be using for various liver injury models which are accompanied by inflammation.

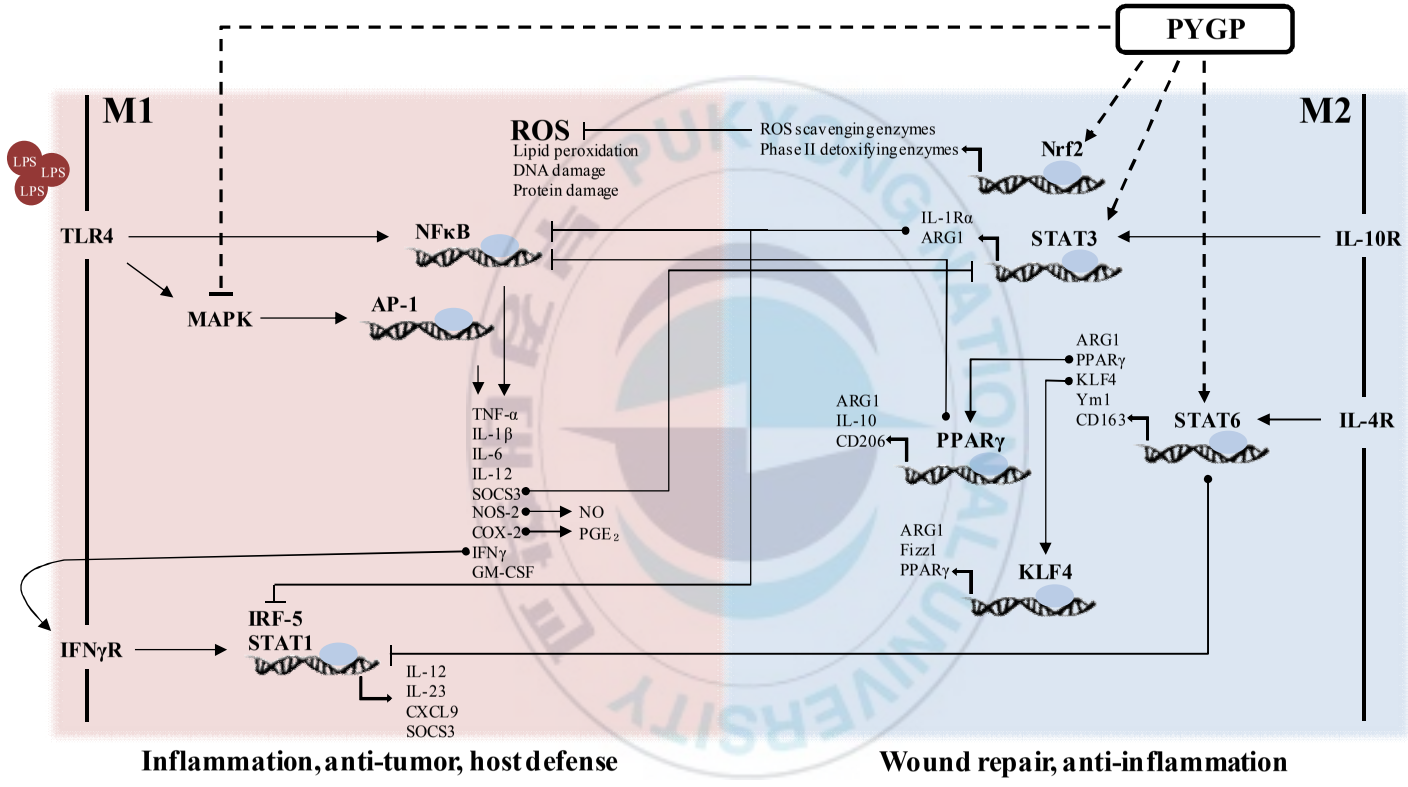

Figure 38. M1 macrophage polarization switch to M2 macrophage by PYGP. Alteration of macrophage polarization through STAT3 and STAT6 transcription factor pathway by PYGP.

Ⅴ. SUMMARY

To investigate the influence of *Pyropia yezoensis* glycoprotein (PYGP) in macrophage M1, M2 phenotype, and liver injury model, experiments were performed using cell and animal models. Macrophages are well-known not only as major regulators of innate and adaptive immunity but also important mediators of systemic metabolism, hematopoiesis, vasculogenesis, apoptosis, malignancy, and reproduction. There are two differentiation patterns, M1 and M2. M1 macrophage (classically activated macrophage) acts as regulator in host defense system. They protect from infection of bacteria, protozoa and virus. M2 macrophage (alternatively activated macrophage) has been reported on anti-inflammatory activity and important in wound healing. This plasticity can change according to macrophages environment. Pre-treatment of PYGP reduced NO, PGE_2, ROS, TBARS, and pro-inflammatory cytokine in LPS-induced M1 activated RAW 264.7 macrophage. In addition, expression of M2 marker (FIZZ1, Ym1, ARG1) was increased during M2 phenotype macrophage metabolism. This phenotype switch was affected STAT3, STAT6 transcription factor activation by PYGP.

Cell and animal models were used to determine the protective effect of PYGP on the liver injury. D-galactosamine (D-GalN) is well known *in vitro* and *in vivo* hepatic injury model. This chemical induces the loss of uridine 5'-triphosphate, uridine 5'-diphosphate, and uridine 5'-monophosphate, moreover inhibits RNA and protein synthesis. In addition, D-GalN-induced oxidative stress is generated through reactive hydroxyl radical damage to the

cell membrane via the stimulation of lipid peroxidation. Expose of D-GalN was induced to cell death in Hepa 1c1c7 cells and D-GalN induced cell death was decreased by pre-treatment of PYGP. PYGP was inhibited oxidative stress and attenuated anti-oxidative enzyme activity by D-GalN. Moreover, it was found to have a protective effect which is the Nrf2 signal pathway activation to be related to inhibit the oxidative stress. This protective effect was found in D-GalN/LPS and chronic ethanol consumption animal model. In the liver injury by D-GalN/LPS and chronic ethanol consumption was recovered by PYGP treatment via MAPK regulation and recover of attenuated anti-oxidative enzymes.

It is accompany inflammation and inhibited antioxidant in liver injury by drug or infection. PYGP was confirmed property of help to liver restoration and switching effect M1 phenotype to M2 phenotype, it has wound healing and anti-inflammatory activity in RAW 264.7 macrophage. These results suggest the possibility of PYGP to be using for various liver injury models which are accompanied by inflammation.

Ⅵ. REFERENCES

Agard, M., Asakrah, S., and Morici, L. A. (2013). PGE_2 suppression of innate immunity during mucosal bacterial infection. *Front Cell Infect Microbiol*, 3, 45.

Aggarwal, B. B. (2004). Nuclear factor-kappaB: The enemy within. *Cancer cell* 6(3), 203-208.

Aliprantis, A. O., Diez-Roux, G., Mulder, L. C., Zychlinsky, A., and Lang, R. A. (1996). Do macrophages kill through apoptosis?. *Immunol Today*, 17(12), 573-576.

Anandan, R., Devi, K. P., Devaki T., and Govindaraju, P. (1998). Preventive effects of *Picrorhiza kurroa* on D-galactosamine-induced hepatitis in rats. *J Clin Biochem Nutr*, 25(2), 87-95.

Aristatile, B., Al-Numair, K. S., Al-Assaf, A. H., and Pugalendi, K. V. (2011). Pharmacological effect of carvacrol on D-galactosamine-induced mitochondrial enzymes and DNA damage by single-cell gel electrophoresis. *J Nat Med*, 65(3-4), 568-577.

Aroor, A. R. and Shukla, S. D. (2004). MAP kinase signaling in diverse effects of ethanol. *Life Sci*, 74(19), 2339–2364.

Bailey, S. M. and Cunningham, C. C. (2002). Contribution of mitochondria to oxidative stress associated with alcoholic liver disease. *Free Radic Biol Med*, 32(1), 11–16.

Barros, M. H. M., Hauck, F., Dreyer, J. H., Kempkes, B., and Niedobitek, G. (2013). Macrophage polarisation: an immunohistochemical

approach for identifying M1 and M2 macrophages. *PLoS One*, 8(11), e80908.

Bindhumol, V., Chitra, K. C., and Mathur, P. P. (2003). Bisphenol A induces reactive oxygen species generation in the liver of male rats. *Toxicology*, 188(2), 117-124.

Biswas, S. K. and Mantovani, A. (2010). Macrophage plasticity and interaction with lymphocyte subsets: cancer as a paradigm. *Nat Immunol*, 11(10), 889-896.

Bosschaerts, T., Guilliams, M., Stijlemans, B., Morias, Y., Engel, D., Tacke, F., Herin, M., Baetselier, P., and Beschin, A. (2010). Tip-DC development during parasitic infection is regulated by IL-10 and requires CCL2/CCR2, IFN-gamma and MyD88 signaling. *PLoS Pathog*, 6(8), e1001045.

Bourel-Bonnet, L., Rao, K. V., Hamann, M. T., and Ganesan, A. (2005). Solid-phase total synthesis of kahalalide A and related analogues. *J Med Chem*, 48(5), 1330-1335.

Brown, B. N., Londono, R., Tottey, S., Zhang, L., Kukla, K. A., Wolf, M. T., Daly, K. A., Reing, J. E., and Badylak, S. F. (2012). Macrophage phenotype as a predictor of constructive remodeling following the implantation of biologically derived surgical mesh materials. *Acta Biomater*, 8(3), 978-987.

Castillo, T., Koop, D. R., Kamimura, S., Triadafilopoulos, G., and Tsukamoto, H. (1992). Role of cytochrome P-450 2E1 in ethanol-, carbon tetrachloride—and iron-dependent microsomal lipid peroxidation. *Hepatology*, 16(4), 992-996.

Cederbaum, A. I. (2010). Role of CYP2E1 in ethanol-induced oxidant stress, fatty liver and hepatotoxicity. *Dig Dis*, 28(6), 802-811.

Ceni, E., Mello, T., and Galli, A. (2014). Pathogenesis of alcoholic liver disease: Role of oxidative metabolism. *World J Gastroenterol*, 20(47), 17756–17772.

Chandini, S. K., Ganesan, P., Suresh, P. V., and Bhaskar, N. (2008). Seaweeds as a source of nutritionally beneficial compounds-a review. *J Food Sci Technol*, 45(1), 1-13.

Chang, T. S., Cho, C. S., Park, S., Yu, S., Kang, S. W., and Rhee, S. G. (2004). Peroxiredoxin III, a mitochondrion-specific peroxidase, regulates apoptotic signaling by mitochondria. *J Biol Chem*, 279(40), 41975–41984.

Chen, L., Ren, F., Zhang, H., Wen, T., Piao, Z., Zhou, L., Zheng, S., Zhang, J., Chen, Y., Han, Y., Duan, Z., and Ma, Y. (2012). Inhibition of glycogen synthase kinase 3β ameliorates D-GalN/LPS-induced liver injury by reducing endoplasmic reticulum stress-triggered apoptosis. *PLoS ONE*, 7(9), e45202.

Chen, Z., Wu, C., Gu, W., Klein, T., Crawford, R., and Xiao, Y. (2014). Osteogenic differentiation of bone marrow MSCs by β-tricalcium phosphate stimulating macrophages via BMP2 signalling pathway. *Biomaterials*, 35(5), 1507-1518.

Cho, D. M., Kim, D. S., Lee, D. S., Kim, H. R., and Pyeun, J. H. (1995). Trace components and functional saccharides in seaweed-1-changes in proximate composition and trace elements according to the harvest season and places. *Bull Korean Fish Soc*, 28(1), 49-59.

Cho, H. I., Park, J. H., Choi, H. S., Kwak, J. H., Lee, D. U., Lee, S. K., and Lee, S. M. (2014). Protective mechanisms of acacetin against D-galactosamine and lipopolysaccharide-induced fulminant hepatic failure in mice. *J Nat Prod*, 77(11), 2497-2503.

Corraliza, I. M., Soler, G., Eichmann, K., and Modolell, M. (1995). Arginase induction by suppressors of nitric oxide synthesis (IL-4, IL-10 and PGE_2) in murine bone-marrow-derived macrophages. *Biochem Biophys Res Commun*, 206(2), 667-673.

Cross, T. G., Scheel-Toellner, D., Henriquez, N. V., Deacon, E., Salmon, M., and Lord, J. M. (2000). Serine/threonine protein kinases and apoptosis. *Exp Cell Res*, 256(1), 34-41.

Das, J., Ghosh, J., Roy, A., and Sil, P. C. (2012). Mangiferin exerts hepatoprotective activity against D-galactosamine induced acute toxicity and oxidative/nitrosative stress via Nrf2–NFκB pathways. *Toxicol Appl Pharmacol*, 260(1), 35-47.

Das, S. K. and Vasudevan, D. M. (2007). Alcohol-induced oxidative stress. *Life Sci*, 81(3), 177-187.

Dawczynski, C., Schubert, R., and Jahreis, G. (2007). Amino acids, fatty acids, and dietary fibre in edible seaweed products. *Food Chem*, 103(3), 891-899.

Decker, K. and Keppler, D. (1971). Galactosamine induced liver injury. *Prog Liver Dis*, 4, 183-199.

El Sayed, K. A., Bartyzel, P., Shen, X., Perry, T. L., Zjawiony, J. K., and Hamann, M. T. (2000). Marine natural products as antituberculosis agents. *Tetrahedron*, 56(7), 949-953.

Ermakova, S., Sokolova, R., Kim, S. M., Um, B. H., Isakov, V., and Zvyagintseva, T. (2011). Fucoidans from brown seaweeds *Sargassum hornery*, *Eclonia cava*, *Costaria costata*: Structural characteristics and anticancer activity. *Appl Biochem Biotechnol*, 164(6), 841-850.

Fenyo, I. M. and Gafencu, A. V. (2013). The involvement of the monocytes/macrophages in chronic inflammation associated with atherosclerosis. *Immunobiology*, 218(11), 1376-1384.

Ferkany, J. W. and Coyle, J. T. (1983). Kainic acid selectively stimulates the release of endogenous excitatory acidic amino acids. *J Pharmacol Exp Ther*, 225(2), 399-406.

Fernandez-Checa, J. C., Ookhtens, M., and Kaplowitz, N. (1987). Effect of chronic ethanol feeding on rat hepatocytic glutathione. Compartmentation, efflux, and response to incubation with ethanol. *J Clin Invest*, 80(1), 57.

Food and Agriculture Organization of the United Nations, Yearbook of Fishery Statistics-Aquaculture Production. http://www.fao.org. (2012).

Fouad, D., Siendones, E., Costán, G., and Muntané, J. (2004). Role of NF-κB activation and nitric oxide expression during PGE_1 protection against D-galactosamine-induced cell death in cultured rat hepatocytes. *Liver Int*, 24(3), 227-236.

Galván-Peña, S. and O'Neill, L. A. (2014). Metabolic reprograming in macrophage polarization. *Front Immunol*, 5.

Gardner, C. R., Heck, D. E., Yang, C. S., Thomas, P. E., Zhang, X. J.,

DeGeorge, G. L., Laskin, J. D., and Laskin, D. L. (1998). Role of nitric oxide in acetaminophen-induced hepatotoxicity in the rat. *Hepatology*, 27(3), 748–754.

Gilani, A. H., Yaeesh, S., Jamal, Q., and Ghayur, M. N. (2005). Hepatoprotective activity of aqueous-methanol extract of Artemisia vulgaris. *Phytother Res*, 19(2), 170-172.

Gordon, S. and Martinez, F. O. (2010). Alternative activation of macrophages: mechanism and functions. *Immunity*, 32(5), 593-604.

Guan, K. L. (1994). The mitogen activated protein kinase signal transduction pathway: from the cell surface to the nucleus. *Cell Signal*, 6(6), 581-589.

Guha, M. and Mackman, N. (2001). LPS induction of gene expression in human monocytes. *Cell Signal*, 13(2), 85-94.

Halliwell, B. (1999). Antioxidant defence mechanisms: from the beginning to the end (of the beginning). *Free Radic Res*, 31(4), 261-272.

Halliwell, B. and Gutteridge, J. (1984). Oxygen toxicity, oxygen radicals, transition metals and disease. *Biochem J*, 219(1), 1-14.

Han, K. H., Hashimoto, N., Shimada, K., Sekikawa, M., Noda, T., Yamauchi, H., Hashimoto, M., Chiji, H., Topping, D. L., and Fukushima, M. (2006). Hepatoprotective effects of purple potato extract against D-galactosamine-induced liver injury in rats. *Biosci Biotechnol Biochem*, 70(6), 1432-1437.

Hard, G. C. (1970). Some biochemical aspects of the immune macrophage. *Br J Exp Pathol*, 51(1), 97-105.

Hines, I. N. and Wheeler, M. D. (2004). Recent advances in alcoholic liver

disease III. Role of the innate immune response in alcoholic hepatitis. *Am J Physiol Gastrointest Liver Physiol*, 287(2), G310–G314.

Holdt, S. L. and Kraan, S. (2011). Bioactive compounds in seaweed: functional food applications and legislation. *J Appl Phycol*, 23(3), 543-597.

Hou, C. C., Huang, C. C., and Shyur, L. F. (2011). *Echinacea* alkamides prevent lipopolysaccharide/D-galactosamine-induced acute hepatic injury through JNK pathway-mediated HO-1 expression. *J Agric Food Chem*, 59(22), 11966-11974.

Hu, K. Q. (2003). Cyclooxygenase 2 (COX2)-prostanoid pathway and liver diseases. *Prostaglandins Leukot Essent Fatty Acids*, 69(5), 329–337.

Hu, X. and Ivashkiv, L. B. (2009). Cross-regulation of signaling pathways by interferon-γ: implications for immune responses and autoimmune diseases. *Immunity*, 31(4), 539-550.

Huang, C. C., Lin, K. J., Cheng, Y. W., Hsu, C. A., Yang, S. S., and Shyur, L. F. (2013). Hepatoprotective effect and mechanistic insights of deoxyelephantopin, a phyto-sesquiterpene lactone, against fulminant hepatitis. *J Nutr Biochem*, 24(3), 516-530.

Hwang, H. J., Kwon, M. J., Kim, I. H., and Nam, T. J. (2008). Chemoprotective effects of a protein from the red algae *Porphyra yezoensis* on acetaminophen-induced liver injury in rats. *Phytother Res*, 22(9), 1149-1153.

Hwang, J. M., Tseng, T. H., Tsai, Y. Y., Lee, H. J., Chou, F. P., Wang,

C. J., and Chu, C. Y. (2005). Protective effects of baicalein on *tert*-butyl hydroperoxide-induced hepatic toxicity in rat hepatocytes. *J Biomed Sci*, 12(2), 389-397.

Inoue, H., Maeda-Yamamoto, M., Nesumi, A., and Murakami, A. (2012). Delphinidin-3-O-galactoside protects mouse hepatocytes from (-)-epigallocatechin-3-gallate-induced cytotoxicity via upregulation of heme oxygenase-1 and heat shock protein 70. *Nutr Res*, 32(5), 357-364.

Ishizaki, M., Kaibori, M., Uchida, Y., Hijikawa, T., Tanaka, H., Ozaki, T., Tokuhara, K., Matsui, K., Kwon, A. H., Kamiyama, Y. (2008). Protective effect of FR183998, a Na^+/H^+ exchanger inhibitor, and its inhibition of iNOS induction in hepatic ischemia-reperfusion injury in rats. *Shock*, 30(3), 311-317.

Jacobson, M. D. (1996). Reactive oxygen species and programmed cell death. *Trends Biochem Sci*, 21(3), 83-86.

Jaeschke, H. (2000). Reactive oxygen and mechanisms of inflammatory liver injury. *J Gastroenterol Hepatol*, 15(7), 718-724.

Jaeschke, H. (2011). Reactive oxygen and mechanisms of inflammatory liver injury: Present concepts. *J Gastroenterol Hepatol*, 26(s1), 173-179.

Jaiswal, A. K. (2004). Nrf2 signaling in coordinated activation of antioxidant gene expression. *Free Radic Biol Med*, 36(10), 1199-1207.

Jemal, A., Bray, F., Center, M. M., Ferlay, J., Ward, E., and Forman, D. (2011). Global cancer statistics. *CA Cancer J Clin*, 61(2), 69-90.

Jeong, Y. I., Jung, I. D., Lee, C. M., Chang, J. H., Chun, S. H., Noh, K. T., Jeong, S. K., Shin, Y. K., Lee, W. S., Kang, M. S., Lee, S.

Y., and Park, Y. M. (2009). The novel role of platelet-activating factor in protecting mice against lipopolysaccharide-induced endotoxic shock. *PLoS One*, 4(8), e6503.

Jiang, Z., Hama, Y., Yamaguchi, K., and Oda, T. (2012). Inhibitory effect of sulphated polysaccharide porphyran on nitric oxide production in lipopolysaccharide-stimulated RAW 264.7 macrophages. *J Biochem*, 151(1), 65-74.

Jin, Q., Jiang, S., Wu, Y. L., Bai, T., Yang, Y., Jin, X., Lian, L., and Nan, J. X. (2014). Hepatoprotective effect of cryptotanshinone from *Salvia miltiorrhiza* in D-galactosamine/lipopolysaccharide-induced fulminant hepatic failure. *Phytomedicine*, 21(2), 141-147.

Johnson, G. L., Dohlman, H. G., and Graves, L. M. (2005). MAPK kinase kinases (MKKKs) as a target class for small-molecule inhibition to modulate signaling networks and gene expression. *Curr Opin Chem Biol*, 9(3), 325-331.

Jones, P. and Suggett, A. (1968). The catalase-hydrogen peroxide system. A theoretical appraisal of the mechanism of catalase action. *Biochem J*, 110, 621-629.

Jurczuk, M. 1., Brzóska, M. M., Moniuszko-Jakoniuk, J., Gałażyn-Sidorczuk, M., and Kulikowska-Karpińska, E. (2004). Antioxidant enzymes activity and lipid peroxidation in liver and kidney of rats exposed to cadmium and ethanol. *Food Chem Toxicol*, 42(3), 429-438.

Kawai, T. and Akira, S. (2007). TLR signaling. *Semin Immunol*, 19(1), 24-32.

Kensler, T. W., Wakabayash, N., and Biswal, S. (2007). Cell survival

responses to environmental stresses via the Keap1-Nrf2-ARE pathway. *Annu Rev Pharmacol Toxicol*, 47, 86-116.

Kilbourn, R. G. and Griffith, O. W. (1992). Overproduction of nitric oxide in cytokine-mediated and septic shock. *J Natl Cancer Inst*, 84(11), 827-831.

Kim, E. K. and Choi, E. J. (2010). Pathological roles of MAPK signaling pathways in human diseases. *Biochim Biophys Acta*, 1802(4), 396-405.

Kim, S. C., Lee, J. R., and Park S. J. (2015). *Porphyra tenera* induces apoptosis of oral cancer cells. *Kor J Herbology*, 30(2), 25-30.

Kim, Y. M., In, J. P., and Park, J. H. (2005). Angiotensin Ⅰ converting enzyme (ACE) inhibitory activities of laver (*Porphyra tenera*) protein hydrolysates. *Prev Nutr Food Sci*, 18(1), 11-18.

Klaassen, C. D. and Reisman, S. A. (2010). Nrf2 the rescue: effects of the antioxidative/electrophilic response on the liver. *Toxicol Appl Pharmacol*, 244(1), 57-65.

Korea Statistical Information Service. http://kosis.kr. (2014).

Krausgruber, T., Blazek, K., Smallie, T., Alzabin, S., Lockstone, H., Sahgal, N., Hussell, T., Feldmann, M., and Udalova, I. A. (2011). IRF5 promotes inflammatory macrophage polarization and TH1-TH17 responses. *Nat Immunol*, 12(3), 231-238.

Kučera, O., Lotková, H., Kanďár, R., Hežová, R., Mužáková, V., and Červinková, Z. (2006). The model of D-galactosamine-induced injury of rat hepatocytes in primary culture. *Acta Medica (Hradec Kralove)*, 49(1), 59-65.

Kumar, K. S., Chu, F. H., Hsieh, H. W., Liao, J. W., Li, W. H., Lin, J. C. C., Shaw, J. F., and Wang, S. Y. (2011). Antroquinonol from ethanolic extract of mycelium of *Antrodia cinnamomea* protects hepatic cells from ethanol-induced oxidative stress through Nrf-2 activation. *J Ethnopharmacol*, 136(1), 168–177.

Kwak, C. S., Kim, S. A., and Lee, M. S. (2005). The correlation of antioxidative effects of 5 Korean common edible seaweeds and total polyphenol content. *J Korean Soc Food Nutr*, 34(8), 1143-1150.

Kwon, M. J. and Nam, T. J. (2006). Porphyran induces apoptosis related signal pathway in AGS gastric cancer cell lines. *Life Sci*, 79(20), 1956-1962.

Labonte, A. C., Tosello-Trampont, A., and Hahn, Y. S. (2014). The role of macrophage polarization in infectious and inflammatory diseases. *Mol Cells*, 37(4), 275-285.

Lau, S. K., Chu, P. G., and Weiss, L. M. (2004). CD163 A specific marker of macrophages in paraffin-embedded tissue samples. *Am J Clin Pathol*, 122(5), 794-801.

Lawrence, T. and Natoli, G. (2011). Transcriptional regulation of macrophage polarization: enabling diversity with identity. *Nat Rev Immunol*, 11(11), 750-761.

Lee, A. S., Jung, Y. J., Kim, D., Nguyen-Thanh, T., Kang, K. P., Lee, S., Park S. K., and Kim, W. (2014). SIRT2 ameliorates lipopolysaccharide-induced inflammation in macrophages. *Biochem Biophys Res Commun*, 450(4), 1363-1369.

Lee, I. K. and Gang, S. W. (1986). A check list of marine algae in Korea. *Algae*, 2, 311-325.

Lee, J. B., Hayashi, K., Hashimoto, M., Nakano, T., and Hayashi, T. (2004). Novel antiviral fucoidan from sporophyll of *Undaria pinnatifida* (Mekabu). *Chem Pharm Bull*, 52(9), 1091-1094.

Lee, J. S., Lee, M. H., and Koo, J. G. (2010). Effects of porphyran and insoluble dietary fiber isolated from laver, *Porphyra yezoensis* on lipid metabolism in rats fed high fat diet. *Kor J Food Nutr*, 23(4), 562-569.

Lekić, N., Cerný, D., Hořínek, A., Provazník, Z., Martínek, J., and Farghali H. (2011). Differential oxidative stress responses to D-galactosamine/lipopolysaccharide hepatotoxicity based on real time PCR analysis of selected oxidant/antioxidant and apoptotic gene expressions in rat. *Physiol Res*, 60(3), 549-558.

Leung, M. T., Lu, Y., Yan, W., Morón-Concepción, J. A., Ward, S. C., Ge, X., Rosa, L. C. D. L., and Nieto, N. (2012). Argininosuccinate synthase conditions the response to acute and chronic ethanol-induced liver injury in mice. *Hepatology*, 55(5), 1596–1609.

Li, R., Yuan, C., Dong, C., Shunang, S., and Choi, M. M. (2011). In vivo antioxidative effect of isoquercitrin on cadmium-induced oxidative damage to mouse liver and kidney. *Naunyn Schmiedebergs Arch Pharmacol*, 383(5), 437-445.

Lim, H. K., Kim, H. S., Choi, H. S., Oh, S., Jang, C. G., Choi, J., Kim, S. H., and Chang, M. J. (2000). Effects of acetylbergenin against D-galactosamine-induced hepatotoxicity in rats. *Pharmacol Res*,

42(5), 471-474.

Lin, S. L., Li, B., Rao, S., Yeo, E. J., Hudson, T. E., Nowlin, B. T., Pei, H. Y., Chen, L., Zheng J. J., Carroll, T. J., Pollard, J. W., Mcmahon, A. P., Lang, R. A., and Duffield, J. S. (2010). Macrophage Wnt7b is critical for kidney repair and regeneration. *Proc Natl Acad Sci*, 107(9), 4194-4199.

Lincoln, R. A., Strupinski, K., and Walker, J. M. (1991). Bioactive compounds from algae. *Life Chem Rep*, 8, 97-183.

Liong, E. C., Xiao, J., Lau, T. Y., Nanji, A. A., and Tipoe, G. L. (2012). Cyclooxygenase inhibitors protect D-galactosamine/lipopolysaccharide induced acute hepatic injury in experimental mice model. *Food Chem Toxicol*, 50(3), 861-866.

Liu, L. and Yeh, Y. Y. (2000). Inhibition of cholesterol biosynthesis by organosulfur compounds derived from garlic. *Lipids*, 35(2), 197-203.

Liu, L. L., Gong, L. K., Qi, X. M., Cai, Y., Wang, H., Wu, X. F., Xiao, Y., and Ren, J. (2005). Altered expression of cytochrome P450 and possible correlation with preneoplastic changes in early stage of rat hepatocarcinogenesis. *Acta Pharmacol Sin*, 26(6), 737-744.

Liu, L. L., Gong, L. K., Wang, H., Xiao, Y., Wu, X. F., Zhang, Y. H., Xue, X., Qi, X. M., and Ren, J. (2008). Baicalin inhibits macrophage activation by lipopolysaccharide and protects mice from endotoxin shock. *Biochem Pharmacol*, 75(4), 914-922.

Livak, K. J. and Schmittgen, T. D. (2001). Analysis of relative gene expression data using real-time quantitative PCR and the $2^{-\Delta\Delta C_T}$

method. *methods*, 25(4), 402-408.

Lopez-Castejón, G., Baroja-Mazo, A., and Pelegrín, P. (2011). Novel macrophage polarization model: from gene expression to identification of new anti-inflammatory molecules. *Cell Mol Life Sci*, 68(18), 3095-3107.

Lu, Y. and Cederbaum, A. I. (2008). CYP2E1 and oxidative liver injury by alcohol. *Free Radic Biol Med*, 44(5), 723–738.

MacDonald, J. R., Thayer, K. J., and White, C. (1987). Inhibition of galactosamine cytotoxicity in an *in vivo*/*in vitro* hepatocellular toxicity model. *Toxicol Appl Pharmacol*, 89(2), 269-277.

MacKinnon, A. C., Farnworth, S. L., Hodkinson, P. S., Henderson, N. C., Atkinson, K. M., Leffler, H., and Sethi, T. (2008). Regulation of alternative macrophage activation by galectin-3. *J Immunol*, 180(4), 2650-2658.

Mallick, N. and Mohn, F. H. (2000). Reactive oxygen species: response of algal cells. *J Plant Physiol*, 157(2), 183-193.

Mandal, P., Pratt, B. T., Barnes, M., McMullen, M. R., and Nagy, L. E. (2011). Molecular mechanism for adiponectin-dependent m2 macrophage polarization link between the metabolic and innate immune activity of full-length adiponectin. *J Biol Chem*, 286(15), 13460-13469.

Mantovani, A., Biswas, S. K., Galdiero, M. R., Sica, A., and Locati, M. (2013). Macrophage plasticity and polarization in tissue repair and remodelling. *J Pathol*, 229(2), 176-185.

Mantovani, A., Garlanda, C., and Locati, M. (2009). Macrophage diversity

and polarization in atherosclerosis a question of balance. *Arterioscler Thromb Vasc Biol*, 29(10), 1419-1423.

Mantovani, A., Sica, A., Sozzani, S., Allavena, P., Vecchi, A., and Locati, M. (2004). The chemokine system in diverse forms of macrophage activation and polarization. *Trends immunol*, 25(12), 677-686.

Martin, K. R. and Barrett, J. C. (2002). Reactive oxygen species as double-edged swords in cellular processes: low-dose cell signaling versus high-dose toxicity. *Hum Exp Toxicol*, 21(2), 71-75.

Martinez, F. O., Helming, L., and Gordon, S. (2009). Alternative activation of macrophages: an immunologic functional perspective. *Annu Rev Immunol*, 27, 451-483.

MatÉs, J. M., Pérez-Gómez, C., and De Castro, I. N. (1999). Antioxidant enzymes and human diseases. *Clin Biochem*, 32(8), 595-603.

Mato, J. M., Cámara, J., de Paz, J. F., Caballería, L., Coll, S., Caballero, A., and Rodés, J. (1999). S-adenosylmethionine in alcoholic liver cirrhosis: a randomized, placebo-controlled, double-blind, multicenter clinical trial. *J Hepatol*, 30(6), 1081-1089.

Morgan, K., French, S. W., and Morgan, T. R. (2002). Production of a cytochrome P450 2E1 transgenic mouse and initial evaluation of alcoholic liver damage. *Hepatology*, 36(1), 122-134.

Munder, M., Eichmann, K., and Modolell, M. (1998). Alternative metabolic states in murine macrophages reflected by the nitric oxide synthase/arginase balance: competitive regulation by $CD4^+$ T cells correlates with Th1/Th2 phenotype. *J Immunol*, 160(11),

5347-5354.

Murakami, A. and Ohigashi, H. (2007). Targeting NOX, INOS and COX-2 in inflammatory cells: Chemoprevention using food phytochemicals. *Int J Cancer Suppl*, 121(11), 2357–2363.

Murray, P. J. (2006). Understanding and exploiting the endogenous interleukin-10/STAT3-mediated anti-inflammatory response. *Curr Opin Pharmacol*, 6(4), 379-386.

Nakagiri, R., Hashizume, E., Kayahashi, S., Sakai, Y., and Kamiya, T. (2003). Suppression by *Hydrangeae Dulcis Folium* of D-galactosamine-induced liver injury *in vitro* and *in vivo*. *Biosci Biotechnol Biochem*, 67(12), 2641-2643.

Nakama, T., Hirono, S., Moriuchi, A., Hasuike, S., Nagata, K., Hori, T., Ido, A., Hayashi, K., and Tsubouchi, H. (2001). Etoposide prevents apoptosis in mouse liver with D-galactosamine/lipopolysaccharide-induced fulminant hepatic failure resulting in reduction of lethality. *Hepatology*, 33(6), 1441-1450.

Nanji, A. A., Khettry, U., Sadrzadeh, S. M., and Yamanaka, T. (1993). Severity of liver injury in experimental alcoholic liver disease. Correlation with plasma endotoxin, prostaglandin E_2, leukotriene B_4, and thromboxane B_2. *Am J Pathol*, 142(2), 367-373.

Nanji, A. A., Miao, L., Thomas, P., Rahemtulla, A., Khwaja, S., Zhao, S., Peters, D., Tahan, S. R., and Dannenberg, A. J. (1997). Enhanced cyclooxygenase-2 gene expression in alcoholic liver disease in the rat. *Gastroenterology*, 112(3), 943–951.

Nathan, C. and Ding, A. (2010). Nonresolving inflammation. *Cell*, 140(6),

871-882.

Nikolic-Paterson, D. J. and Atkins, R. C. (2001). The role of macrophages in glomerulonephritis. *Nephrol Dial Transplant*, 16(5), 3-7.

Noda, H. (1993). Health benefits and nutritional properties of nori. *J Appl Psychol*, 5(2), 255-258.

Nordberg, J. and Arnér, E. S. (2001). Reactive oxygen species, antioxidants and the mammalian thioredoxin system. *Free Radic Biol Med*, 31(11), 1287-1312.

Nordmann, R., Ribière, C., and Rouach, H. (1992). Implication of free radical mechanisms in ethanol-induced cellular injury. *Free Radic Biol Med*, 12(3), 219-240.

oshizawa, Y., Ametani, A., Tsunehiro, J., Nomura, K., Itoh, M., Fukui, F., and Kaminogawa, S. (1995). Macrophage stimulation activity of the polysaccharide fraction from a marine alga (*Porphyra yezoensis*): structure-function relationships and improved solubility. *Biosci Biotechnol Biochem*, 59(10), 1933-1937.

Ostrowska, J., Łuczaj, W., Kasacka, I., Różański, A., and Skrzydlewska, E. (2004). Green tea protects against ethanol-induced lipid peroxidation in rat organs. *Alcohol*, 32(1), 25–32.

Osumi, Y., Kawai, M., Amano, H., and Noda, H. (1998). Antitumor activity of oligosaccharides derived from *Porphyra yezoensis* porphyran. *Bull Jpn Soc Sci Fish*.

Pal, A., Mohit CK., and Ajay K. (2014). Bioactive Compounds and Properties of Seaweeds—A Review. *Jourlib Journal* 1, e752.

Park, H. M., Kim, S. J., Mun, A. R., Go, H. K., Kim, G. B., Kim, S. Z.,

Jang, S. I., Lee, S. J., Kim, J. S., and Kang, H. S. (2012). Korean red ginseng and its primary ginsenosides inhibit ethanol-induced oxidative injury by suppression of the MAPK pathway in TIB-73 cells. *J Ethnopharmacol*, 141(3), 1071–1076.

Park, S. J., Park, C. I., and Kim, S. C. (2010). Antimicrobial activities of ethanolic extracts of marine resources against *Propionibacterium acnes*. *Kor J Herbology*, 25(2), 65-70.

Pearson, G., Robinson, F., Beers Gibson, T., Xu, B. E., Karandikar, M., Berman, K., and Cobb, M. H. (2001). Mitogen-activated protein (MAP) kinase pathways: regulation and physiological functions 1. *Endocr Rev*, 22(2), 153-183.

Prasse, A., Germann, M., Pechkovsky, D. V., Markert, A., Verres, T., Stahl, M., Melchers, L., Luttmann, W., Muller-Quernheim, M., and Zissel, G. (2007). IL-10–producing monocytes differentiate to alternatively activated macrophages and are increased in atopic patients. *J Allergy Clin Immunol*, 119(2), 464-471.

Pushpavalli, G., Kalaiarasi, P., Veeramani, C., and Pugalendi, K. V. (2010). Effect of chrysin on hepatoprotective and antioxidant status in D-galactosamine-induced hepatitis in rats. *Eur J Pharmacol*, 631(1), 36-41.

Quan, J., Yin, X., and Xu, H. (2011). *Boschniakia rossica* prevents the carbon tetrachloride-induced hepatotoxicity in rat. *Exp Toxicol Pathol*, 63(1), 53–59.

Raes, G., De Baetselier, P., Noël, W., Beschin, A., Brombacher, F., and Gh, G. H. (2002). Differential expression of FIZZ1 and Ym1 in

alternatively versus classically activated macrophages. *J Leukoc Biol*, 71(4), 597-602.

Rajendrasozhan, S., Periyaswamy, V., and Kodukkur, V. P. (2006). Protective effect of ursolic acid on ethanol-mediated experimental liver damage in rats. *Life Sci*, 78(7), 713–718.

Ricote, M., Welch, J. S., and Glass, C. K. (2000). Regulation of macrophage gene expression by the peroxisome proliferator-activated receptor-γ. *Horm Res Paediatr*, 54(5-6), 275-280.

Rouach, H., Fataccioli, V., Gentil, M., French, S. W., Morimoto, M., and Nordmann, R. (1997). Effect of chronic ethanol feeding on lipid peroxidation and protein oxidation in relation to liver pathology. *Hepatology*, 25(2), 351-355.

Sakaguchi, S. and Yokota, K. (1995). Role of Ca^{2+} on Endotoxin-Sensitivity by Galactosamine Challenge: Lipid Peroxide Formation and Hepatotoxicity in Zymosan-Primed Mice. *Pharmacol Toxicol*, 77(2), 81-86.

Schaeffer, D. J. and Krylov, V. S. (2000). Anti-HIV activity of extracts and compounds from algae and cyanobacteria. *Ecotoxicol Environ Saf*, 45(3), 208-227.

Scott, R. B., Reddy, K. S., Husain, K., Schlorff, E. C., Rybak, L. P., and Somani, S. M. (2000). Dose response of ethanol on antioxidant defense system of liver, lung, and kidney in rat. *Pathophysiology*, 7(1), 25-32.

Scotton, C. J., Martinez, F. O., Smelt, M. J., Sironi, M., Locati, M.,

Mantovani, A., and Sozzani, S. (2005). Transcriptional profiling reveals complex regulation of the monocyte IL-1β system by IL-13. *J Immunol*, 174(2), 834-845.

Sen, A. K., Das, A. K., Banerji, N., Siddhanta, A. K., Mody, K. H., Ramavat, B. K., and Ganguly, D. K. (1994). A new sulfated polysaccharide with potent blood anti-coagulant activity from the red seaweed *Grateloupia indica*. *Int J Biol Macromol*, 16(5), 279-280.

Serbina, N. V., Salazar-Mather, T. P., Biron, C. A., Kuziel, W. A., and Pamer, E. G. (2003). TNF/iNOS-producing dendritic cells mediate innate immune defense against bacterial infection. *Immunity*, 19(1), 59-70.

Serhan, C. N. and Oliw, E. (2001). Unorthodox routes to prostanoid formation: New twists in cyclooxygenase-initiated pathways. *J Clin Invest*, 107(12), 1481-1489.

Seth, D., Haber, P. S., Syn, W. K., Diehl, A. M., and Day, C. P. (2011). Pathogenesis of alcohol-induced liver disease: Classical concepts and recent advances. *J Gastroenterol Hepatol*, 26(7), 1089–1105.

Shi, Y., Sun, J., He, H., Guo, H., and Zhang, S. (2008). Hepatoprotective effects of *Ganoderma lucidum* peptides against D-galactosamine-induced liver injury in mice. *J Ethnopharmacol*, 117(3), 415-419.

Shin, E. S., Hwang, H. J., Kim, I. H., and Nam, T. J. (2011). A glycoprotein from *Porphyra yezoensis* produces anti-inflammatory effects in liposaccharide-stimulated macrophages via the TLR4

signaling pathway. *Int J Mol Med*, 28(5), 809-815.

Sica, A. and Mantovani, A. (2012). Macrophage plasticity and polarization: *in vivo* veritas. *J Clin Invest*, 122(3), 787-795.

Sica, A., Invernizzi, P., and Mantovani, A. (2014). Macrophage plasticity and polarization in liver homeostasis and pathology. *Hepatology*, 59(5), 2034-2042.

Stengel, D. B., Connan, S., and Popper, Z. A. (2011). Algal chemodiversity and bioactivity: sources of natural variability and implications for commercial application. *Biotechnol Adv*, 29(5), 483–501.

Tahir, M., Rehman, M. U., Lateef, A., Khan, R., Khan, A. Q., Qamar, W., Ali, F., O'hamiza, O., and Sultana, S. (2013). Diosmin protects against ethanol-induced hepatic injury via alleviation of inflammation and regulation of TNF-α and NF-κB activation. *Alcohol*, 47(2), 131–139.

Tak, P. P. and Firestein, G. S. (2001). NF-kappaB: A key role in inflammatory diseases. *J Clin Invest*, 107(1), 7-11.

Tang, X. H., Gao, L., Gao, J., Fan, Y. M., Xu, L. Z., Zhao, X. N., and Xu, Q. (2004). Mechanisms of hepatoprotection of *Terminalia catappa* L. extract on D-galactosamine-induced liver damage. *Am J Chin Med*, 32(04), 509-519.

Trinchero, J., Ponce, N., Córdoba, O. L., Flores, M. L., Pampuro, S., Stortz, C. A., Salomon, H., and Turk, G. (2009). Antiretroviral activity of fucoidans extracted from the brown seaweed *Adenocystis utricularis*. *Phytother Res*, 23(5), 707-712.

Tugal, D., Liao, X., and Jain, M. K. (2013). Transcriptional control of

macrophage polarization. *Arterioscler Thromb Vasc Biol*, 33(6), 1135-1144.

Venugopal, S. K., Chen, J., Zhang, Y., Clemens, D., Follenzi, A., and Zern, M. A. (2007). Role of MAPK phosphatase-1 in sustained activation of JNK during ethanol-induced apoptosis in hepatocyte-like VL-17A cells. *J Biol Chem*, 282(44), 31900-31908.

Verreck, F. A., de Boer, T., Langenberg, D. M., Hoeve, M. A., Kramer, M., Vaisberg, E., Kastelein, R., Kolk, A., Waal-Malefyt, R. D., and Ottenhoff, T. H. (2004). Human IL-23-producing type 1 macrophages promote but IL-10-producing type 2 macrophages subvert immunity to (myco) bacteria. *Proc Natl Acad Sci U S A*, 101(13), 4560-4565.

Vimal, V. and Devaki, T. (2004). Hepatoprotective effect of allicin on tissue defense system in galactosamine/endotoxin challenged rats. *J Ethnopharmacol*, 90(1), 151-154.

Visser, K. E., Korets, L. V., and Coussens, L. M. (2005). De novo carcinogenesis promoted by chronic inflammation is B lymphocyte dependent. *Cancer cell*, 7(5), 411-423.

Wada, T. and Penninger, J. M. (2004). Mitogen-activated protein kinases in apoptosis regulation. *Oncogene*, 23(16), 2838–2849.

Wang, H., Xu, D. X., Lv, J. W., Ning, H., and Wei, W. (2007). Melatonin attenuates lipopolysaccharide (LPS)-induced apoptotic liver damage in D-galactosamine-sensitized mice. *Toxicology*, 237(1), 49-57.

Wang, N., Liang, H., and Zen, K. (2014). Molecular mechanisms that influence the macrophage M1–M2 polarization balance. *Front*

Immunol, 5, 614.

Wang, Y., Gao, L. N., Cui, Y. L., and Jiang, H. L. (2014). Protective effect of danhong injection on acute hepatic failure induced by lipopolysaccharide and D-galactosamine in mice. *Evid Based Complement Alternat Med*, 2014, ID153902, 8.

Wei, L., Ren, F., Zhang, X., Wen, T., Shi, H., Zheng, S., Zhang, J., Chen, Y., Han, Y., and Duan, Z. (2014). Oxidative stress promotes D-GalN/LPS-induced acute hepatotoxicity by increasing glycogen synthase kinase 3β activity. *Inflamm Res*, 63(6), 485-494.

Wen, T., Wu, Z. M., Liu, Y., Tan, Y. F., Ren, F., and Wu, H. (2007). Upregulation of heme oxygenase-1 with hemin prevents D-galactosamine and lipopolysaccharide-induced acute hepatic injury in rats. *Toxicology*, 237(1), 184-193.

West, A. P., Brodsky, I. E., Rahner, C., Woo, D. K., Erdjument-Bromage, H., Tempst, P., Walsh, M. C., Choi, Y., Shadel G. S., and Ghosh, S. (2011). TLR signalling augments macrophage bactericidal activity through mitochondrial ROS. *Nature*, 472(7344), 476-480.

Wilhelm, E. A., Jesse, C. R., Roman, S. S., Nogueira, C. W., and Savegnago, L. (2009). Hepatoprotective effect of 3-alkynyl selenophene on acute liver injury induced by D-galactosamine and lipopolysaccharide. *Exp Mol Pathol*, 87(1), 20-26.

Wu, G., Fang, Y. Z., Yang, S., Lupton, J. R., and Turner, N. D. (2004). Glutathione metabolism and its implications for health. *J Nutr*, 134(3), 489–492.

Wu, K. C., Cui, J. Y., and Klaassen, C. D. (2012). Effect of graded Nrf2 activation on phase-I and II drug metabolizing enzymes and transporters in mouse liver. *Plos One*, 7, e39006.

Xia, X., Su, C., Fu, J., Zhang, P., Jiang, X., Xu, D., Hu, L., Song, E., and Song, Y. (2014). Role of α-lipoic acid in LPS/D-GalN induced fulminant hepatic failure in mice: Studies on oxidative stress, inflammation and apoptosis. *Int Immunopharmacol*, 22(2), 293-302.

Xu, H., Barnes, G. T., Yang, Q., Tan, G., Yang, D., Chou, C. J., Sole, J., Nichols, A., Ross, J. S., Tartaglia, L. A., and Chen, H. (2003). Chronic inflammation in fat plays a crucial role in the development of obesity-related insulin resistance. *J Clin Invest*, 112(12), 1821-1830.

Yu, K. X., Jantan, I., Ahmad, R., and Wong, C. L. (2014). The major bioactive components of seaweeds and their mosquitocidal potential. *Parasitol Res*, 113(9), 3121-3141.

Zhang, Q., Li, N., Liu, X., Zhao, Z., Li, Z., and Xu, Z. (2004). The structure of a sulfated galactan from *Porphyra haitanensis* and its *in vivo* antioxidant activity. *Carbohydr Res*, 339(1), 105-111.

Zhang, Z., Zhang, Q., Wang, J., Song, H., Zhang, H., and Niu, X. (2010). Regioselective syntheses of sulfated porphyrans from *Porphyra haitanensis* and their antioxidant and anticoagulant activities *in vitro*. *Carbohydr Polym*, 79(4), 1124-1129.

Zhou, G., Sun, Y., Xin, H., Zhang, Y., Li, Z., and Xu, Z. (2004). *In vivo* antitumor and immunomodulation activities of different molecular weight lambda-carrageenans from *Chondrus ocellatus*. *Pharmacol*

Res, 50(1), 47-53.

Zima, T. and Kalousova, M. (2005). Oxidative stress and signal transduction pathways in alcoholic liver disease. *Alcohol Clin Exp Res*, 29(s2), 110S–115S.